July 2021

Structural Shielding Considerations for VMAT

Ana Lucia Dieguez
Louisiana State University and Agricultural and Mechanical College

STRUCTURAL SHIELDING CONSIDERATIONS FOR VMAT

A Thesis

Submitted to the Graduate Faculty of the
Louisiana State University and
Agricultural and Mechanical College
in partial fulfillment of the
requirements for the degree of
Master of Science

in

The Department of Physics and Astronomy

by
Ana Lucia Dieguez
B.S., Universidad del Valle de Guatemala, 2017
August 2021

This work is dedicated to my parents
who on a cold October morning,
left behind their country and life
so that I'd have a better chance at mine

Acknowledgments

Many people were instrumental in the completion of this project, and I want to thank them. First, I want to thank my advisor Kip Matthews, for teaching me and guiding me through all my research journey, and for giving me the opportunity to pursue a project that not many would've liked to advise on. I want to thank my committee members Dan Neck, Jonas Fontenot, and Scott Marley for all their time and feedback provided. I especially thank Dan Neck for offering his years of experience in shielding design, answering all my questions, and for helping me troubleshoot equipment while I had limited access to the clinic.

I would like to thank the Kenneth R. Hogstrom Superior Graduate Student Scholarship in Medical Physics from the Louisiana State University in coalition with Mary Bird Perkins Cancer Center's Medical Physics Program, for providing essential funding for this project. To Dr. Kenneth Hogstrom, a special thank you for the support offered to LSU's medical physics students through the creation of this scholarship. To the LSU Medical Physics Program and its faculty members: thank you for all their shared knowledge, mentoring, and for all the "you need to know these for the rest of your career". I want to express my gratitude to Katelynn Fontenot, Yao Zeng, Sussan Hammond, and Paige Whittington for all the administrative support and guidance.

Thank you to my student colleagues for making graduate school a memorable experience, but specially to Joseph Scotto, Stephanie Wang, Jared Taylor, Chie Lung, Ivan Hidrovo and Maryam Naseri for their friendship. A special thank you to Joseph and Michael for their support while navigating the last year of research with me. To my husband Charles LeBlanc, my sisters, and my parents thank you for the encouragement and moral support. I want to specially thank my dad, for putting his doubts aside and supporting me in my decision to become a physicist instead of an engineer.

Table of contents

Abstract

Introduction: As noted in National Council on Radiation Protection and Measurements (NCRP) Report 151, the medical physicist or other qualified expert has the responsibility to keep abreast of any new technology or treatment method that could potentially impact structural shielding design. Volumetric arc therapy (VMAT) became prevalent after the publication of Report 151 and thus was not explicitly addressed in Report 151. If the shielding-related characteristics of VMAT differ enough from the expectations of Report 151, especially in the circumstance of a vault utilized exclusively for VMAT, a shielding design based on Report 151 could potentially be inadequate. The goal of this work was (1) to assess the characteristics of VMAT deliveries that potentially impact shielding design, and (2) to determine if Report 151, as published and incorporating only minimal conservative design choices, will result in a safe shielding design for a dedicated VMAT treatment vault. Three shielding parameters were characterized: workload, VMAT modulation factor, and use factors.

Materials and Methods: A secondary verification system, MobiusLog (Mobius Medical Systems, LP, Houston, TX) was used to obtain real-time mechanical tracking of VMAT deliveries on five linear accelerators at three facilities over a 4-month period. After anonymization, these log files were analyzed by individual accelerators and by type of treatment site (e.g., chest, head & neck, prostate), as well as collectively. The fractionation scheme for each patient was used to compute weekly workloads and VMAT modulation factors. Use factors were determined from reported gantry positions during treatment, for 90° (conventional), 45° (IMRT), 30°, and 15° angular binning intervals, and compared to Report 151. Using the VMAT-specific parameters, shielding was designed for a sample vault; these barriers were compared to barriers designed with parameters from Report 151.

Results: Workloads derived from the log files agreed with independent clinic records, indicating the log files contained complete delivery information. Composited over all accelerators and treatment sites, the use factors were essentially uniformly distributed around the full circle; deviations from uniform were most noticeable at the smaller binning intervals and for the 0° (beam directed at floor) and 180° (beam directed at ceiling) intervals. The use factors per treatment site were also relatively uniformly distributed, except for lung and chest sites. The sample vault design showed that the Report 151 use factors occasionally underestimated barrier requirements compared to log file-based VMAT use factors or the assumption of uniform gantry rotation. The inclusion of reasonable conservative margins on calculations may allow Report 151-based barriers to be adequately safe. A tapered ceiling barrier that is designed using Report 151's 45° (IMRT) interval use factors will not yield a safe shielding design. The VMAT-specific data should not significantly impact the design calculations for secondary barriers or doors, primarily because these barriers are independent of use factor.

Conclusion: The VMAT-specific use factors reported in this work, as well as the assumption of uniformly-distributed use factors, consistently led to primary barrier thicknesses that were at least as safe as those calculated from published Report 151 use factors. Shielding calculations based on Report 151 can produce adequate primary barriers for a dedicated VMAT vault only if the qualified expert incorporates sufficient conservative overestimates, i.e., enough to compensate for the larger VMAT use factors, in some barriers. A tapered ceiling barrier in a dedicated VMAT vault should be designed using either VMAT-specific use factors or assumed uniformly-distributed use factors, not the published 45° (IMRT) interval use factors of Report 151. The assumption of uniformly distributed use factors is reasonable for designing a general-purpose VMAT vault, but

treatment site-specific use factors should be used to design a vault that will be used heavily for only one (or a few) treatment sites, such as chest or lung.

Chapter 1. Introduction

This chapter presents the motivation and background information pertinent to this research work. The motivation describes the importance of assessing the potential impact of newly developed radiotherapy treatment methods on current structural shielding design methods. The background reviews the current state of practice for structural shielding design as well as the radiotherapy treatment approach of volumetric arc therapy (VMAT). The chapter concludes with the hypothesis and specific aims of this work.

1.1. Motivation

The goal of radiation protection is to minimize the likelihood of radiation-induced harm to radiation workers and the general public (NCRP, 1993). Medical physicists and similar qualified experts use three principles to reduce radiation exposure: time, distance, and shielding. In a megavoltage clinical radiotherapy facility, the time spent near and the distance from a radiation source are often dictated by facility operations; therefore, physical shielding is the primary tool to minimize the exposure of radiation workers and the general public alike. The National Council on Radiation Protection and Measurements (NCRP) is the primary entity in the U.S. that recommends procedures for the design of structural shielding. The NCRP brings together representatives of government, industry, academia and other stakeholders to offer consensus guidelines and summary information related to radiation protection practices (NCRP, 2019).

In 2005, the NCRP delineated the most recent recommendations for the design of structural shielding for megavoltage x-ray and gamma-ray radiotherapy facilities in Report 151 (NCRP, 2005). These guidelines were based on the clinical radiation delivery modalities that were common at the time of publication. The constantly evolving nature of radiation delivery methods makes it the responsibility of the medical physicist or other qualified expert to keep abreast of any new

technology that could potentially impact structural shielding design (NCRP, 2005). One recent development not included in NCRP Report 151 is volumetric arc therapy (VMAT). This modality has quickly become the predominant treatment delivery for tumor sites like prostate, head and neck, and breast. (Teoh, Clark, Wood, Whitaker, & Nisbet, 2011). VMAT has seen rapid and widespread adoption because this technology can be implemented on a conventional clinical linear accelerator that is already equipped with multileaf collimators for intensity-modulated radiation therapy (IMRT). No specialized radiation source or geometry is required, unlike tomotherapy (Robinson, Scrimger, Field, & Fallone, 2000), robotic arm systems (Rodgers, 2005), or gamma knife (McDermott, 2007). With fast and accurate delivery of arcs (Teoh et al., 2011), and easy implementation, most facilities have upgraded their accelerators to also deliver VMAT treatments.

Few attempts have been made to analyze the impact that arc therapy has on the various parameters for the design of structural shielding (Teoh et al., 2011). No reports have been found in the literature of IMRT treatment vaults being inadequate for VMAT. Two possible reasons are (1) conservative margins added onto designs have fortuitously been sufficient for VMAT, and (2) any potentially inadequate vaults were remediated but the effort was not written up for publication. In any case, Report 151 does not explicitly account for VMAT deliveries and thus potentially could result in an inadequate vault design *especially in the circumstance of a vault utilized exclusively for VMAT*. Therefore, this thesis work will characterize VMAT deliveries relative to shielding design parameters and analyze their potential impact on Report 151-based shielding design. This work will recommend modified procedures and provide supplemental data that may be used by other qualified experts to design new treatment vaults or to evaluate existing vaults for substantial use of VMAT.

1.2. Background

1.2.1. History of radiation protection and NCRP

The discovery of x-rays and radioactive processes in the late 19th century revolutionized the medical imaging field. Not long after its discovery, radiation proved to be beneficial as a curative method, and soon after started to be implemented in all sorts of therapeutic modalities (Inkret, Meinhold, & Taschner, 1995). While radiation was found to be beneficial, adverse effects were soon observed (Grossman, 1982); this served as the early motivation for physicists to create radiation protection societies in the U.S. and elsewhere (Inkret et al., 1995). These societies sought to develop and promulgate guidelines for the safe use of radiation. The societies in the U.S. eventually developed into the National Council for Radiation Protection and Measurements (NCRP 151, 2005). In 1993 the NCRP published Report 116 which proposed the current limit for radiation exposure in the United States; for radiation workers, the annual exposure limit is 50 mSv/year while the general public is limited to 1 mSv/year (NCRP, 1993). In 2005, the NCRP published Report 151, the current guidelines for structural radiation shielding design of radiotherapy facilities (NCRP, 2005).

1.2.2. NCRP Report 151: Structural Shielding Design and Evaluation for Megavoltage X- and Gamma-ray Radiotherapy Facilities

Report 151 presents the current recommendations related to the design and installation of structural shielding at megavoltage radiotherapy facilities (NCRP, 2005). This publication consolidated, revised, and extended the shielding design recommendations in Report 49 (NCRP, 1976), Report 51 (NCRP, 1977), and Report 79 (NCRP, 1986). Report 151 included IMRT treatment methods which had become widespread in the preceding decade. Report 151 presents methods and supplemental data to calculate required barrier thicknesses to keep potential radiation

exposures of workers and the public below regulatory limits. The following paragraphs review the Report 151 formalism.

The purpose of a radiation barrier is to attenuate any radiation incident on the barrier, to bring the *dose equivalent (H)* beyond the barrier to or below acceptable limits. Called the *design goal (P)*, these limits are based on regulatory limits (10 C.F.R. § 20, 1991) and ALARA practice; NCRP sets design goals of 0.1 mSv/week for radiation workers and 0.02 mSv/week for the general public. Barrier thickness per Report 151 depends on the type and magnitude of radiation that is incident on the barrier, as well as characteristics of the area that is being protected. Walls, ceiling, floor, and door in a linac vault all serve as shielding barriers.

A barrier that sees direct incidence of the therapeutic field from the radiation source is designated a primary barrier. The shielding parameters necessary to calculate primary barrier thickness are:

- *Workload (W)* which is the weekly average photon absorbed dose delivered to isocenter. (See Report 151 for additional stipulations)
- *Use factor (U)* which is the fraction of the workload that is delivered towards a given primary barrier
- *Distance (d)* which is the distance from the source to the point of protection beyond the barrier. Radiation intensity decreases with distance based on the inverse square law; Report 151 stipulates that the closest a protected person's critical organs can get to the barrier for a significant amount of time is 0.3 m
- *Occupancy factor (T)* which is the fraction of time that the protected person is present beyond the barrier

With reference to the design goal, these shielding parameters yield the barrier's *transmission factor* (*B*). The transmission factor is the ratio of the design goal (dose equivalent allowed) to the radiation reaching the point of protection with no barrier present. Therefore, the transmission factor for a primary barrier is given by:

$$B_{pri} = \frac{Pd^2}{WUT} \qquad \text{(Eq. 1)}$$

and represents the fraction to which the barrier shielding must attenuate the primary beam.

A secondary barrier is the one that does not see direct incidence of the radiation beam but can receive leakage radiation from the source, scattered radiation from the patient and treatment apparatus (and from walls in some circumstances), and photoneutrons and neutron-capture gamma rays. Photoneutrons and neutron-capture gamma rays only become a concern for shielding design when the linac's operating potential is above 10 MV, and thus are not a concern for VMAT (NCRP, 2005). Arising from primary radiation, scatter and leakage magnitudes at the point of protection are derived from workload (Kermani, Leclerc, Martel, & Fareh, 2001; NCRP, 2005). Because scatter and leakage are produced whenever the source is energized and are emitted in all directions regardless of the direction in which the gantry points, the use factor for secondary radiation is always 1. A properly designed primary barrier is sufficient to also shield any secondary radiation incident upon it (NCRP, 2005), because secondary radiation is potentially several orders of magnitude lower in intensity than the primary beam workload.

To calculate the dose equivalent due to scatter at the point of protection beyond a secondary barrier, several shielding parameters are required in addition to workload. These are:

- *Scatter distance (d_{sca})* which is the distance from the radiation source to the scattering site

- *Secondary distance (d_{sec})* which is the distance from the scattering site to the point of protection located 0.3 m past the barrier
- *Scatter fraction (a)* which is the fraction of the workload that scatters from the patient in the direction of the barrier; scatter fraction is tabulated in Report 151 for a 20x20 cm^2 treatment field
- *Field area (F)* which is the area of the treatment field, measured at isocenter (usually 1 m from the source)

The transmission factor required from the barrier to reduce scatter at the point of protection to the design goal is given by:

$$B_{ps} = \frac{P}{aWT} d_{sca}^2 d_{sec}^2 \frac{400}{F} \qquad \text{(Eq. 2)}$$

Leakage radiation is due to penetration of stray radiation through the shielding around the linac source. Manufacturers are required to provide head shielding that attenuates no less than 99.9% of this stray radiation, i.e., only 0.1% is incident on structural barriers (NCRP, 1989); the head shielding thus has a transmission factor of 10^{-3}.

The amount of leakage is proportional to the total radiation produced by the accelerator to achieve the desired workload at isocenter; some treatment techniques may require substantially more radiation production by the accelerator compared to the workload measured at isocenter. For instance, treatment techniques like IMRT and VMAT stitch together many small collimated fields, blocking much of the primary beam at any moment but still contributing to leakage. Therefore, for modulated radiation therapy, the leakage workload needs to be accounted for. In Report 151, *Leakage factor (C)* is defined as the ratio of monitor units (MU) needed to deliver 1 cGy to isocenter with small blocked fields to the MU needed to deliver 1 cGy to isocenter with a large

open field. For IMRT, the higher monitor units produced to deliver a prescribed dose per patient when compared to an open field beam is:

$$MU_{IMRT} = \sum_i \frac{MU_i}{D_{pre\,i}} \qquad \text{(Eq. 3)}$$

and the *leakage factor (C_I),* also known as IMRT factor (NCRP, 2005) is thus:

$$C_I = \frac{MU_{IMRT}}{MU_{conv}} \qquad \text{(Eq. 4)}$$

The dose equivalent at the point of protection due to leakage thus depends, in addition to workload, the mandatory head transmission of 10^{-3}, and leakage factor, on:

- *Leakage distance (d_L)* which is the distance from the source to the point of protection located 0.3 m beyond the secondary barrier. This distance can be measured from isocenter in some circumstances (NCRP, 2005).

Therefore, the leakage transmission factor is given by:

$$B_L = \frac{Pd^2}{10^{-3}CWT} \qquad \text{(Eq. 5)}$$

for modulated fields. For an unmodulated (open) field, C=1 and the leakage workload is the same as the primary workload.

Once the transmission factors are computed, the thickness of both primary and secondary barriers is determined based from the operating energy of the accelerator and the type of material that will be used in the barrier. For convenience, the attenuating properties of materials are characterized by the tenth value layer (TVL), rather than the more familiar attenuation coefficient for exponential attenuation. One TVL of material attenuates a radiation beam to one-tenth of its initial value. The *number of TVLs (n)* needed to attenuate the beam to the design goal is derived from the transmission factor as:

$$n = -\log(B) \quad \text{(Eq. 6)}$$

Report 151 tabulates TVLs for commonly used materials such as concrete and lead, for a range of common operating voltages.

The bremsstrahlung x-rays produced by a radiotherapy linear accelerator are polychromatic. Due to spectral changes in this radiation as it passes through the barrier, the effective attenuation coefficient is not constant. For shielding purposes, more material is required to achieve the first 10x reduction in beam intensity (TVL_1), compared to subsequent reductions (TVL_e). The thickness of a barrier that requires *n* TVLs therefore is defined by:

$$t_{barrier} = TVL_1 + (n-1)TVL_e \quad \text{(Eq. 7)}$$

Prior to Report 151, several research studies showed that IMRT techniques had a leakage workload two to three times greater than a conventional 4-field delivery (Mechalakos, Germain, & Burman, 2004). A higher leakage workload directly increases the required thicknesses of all secondary barriers. However, particular treatment techniques may affect specific barriers, such as by altering the numbers and directions of treatment beams relative to conventional methods. The impact of new treatment techniques such as VMAT on shielding design must be assessed, to ensure that both existing and new vaults are certain to protect radiation workers and the public.

1.2.3. Volumetric Arc Therapy

Modulated field deliveries were a solution to many tumor conformality issues while sparing at risk structures near the treated site (Teoh et al., 2011). Intensity modulated radiotherapy (IMRT) relies on field modulation through multi leaf collimators (MLCs) in the beam's path to conform to a structure, while sparing close-by organs. IMRT also uses variable dose delivery across beamlets to achieve dose conformality to the tumor while also implementing different beam positions

around the patient. Each beam can deliver a different modulated field at each step; hence this delivery method is called step-and-shoot delivery (Yu & Tang, 2011).

A standard IMRT plan often requires multiple fixed angle radiation beams, which increases treatment delivery time. Better conformality requires more beams and more complex treatment plans, which makes IMRT not only time consuming to deliver the plan itself, but also time consuming to plan. To improve the complexity and long treatment times, in 1995 Yu proposed the idea of intensity modulated arc therapy (IMAT) (Yu, 1995). Arc therapy is based on the concept of delivering radiation by rotating the radiation source at a full 360º beam angle. When it was first proposed, IMAT relied on the use of multiple arcs superimposed to achieve conformality while still modulating the field via MLCs (Yu, 1995).

Arc therapy continuously delivers radiation while adapting the beam's field shape to the tumor's shape (Khan, 2014). However, when IMAT was first introduced the available technology had limitations, and several different approaches were used to achieve the superposition of arcs with little success of becoming commercialized (Yu & Tang, 2011). In 2008, volumetric arc therapy (VMAT) was introduced as a single-arc IMAT technique that could achieve dose rate variation with different segment weights throughout a single-arc rotation (Otto, 2008). VMAT simultaneously varies three parameters during the beam deliver: gantry speed, aperture shape (via MLCs), and dose rate; VMAT soon became rapidly commercialized (Otto, 2008). Nowadays, the entire treatment volume can be treated with one or two arcs, although more complex cases may use more arcs (Teoh et al., 2011).

1.2.4. Impact of VMAT on shielding design

Occurring after the publication of Report 151, volumetric arc therapy (VMAT) has now been widely implemented in radiotherapy facilities and has also become the predominant treatment

delivery method for tumor sites like prostate, head and neck, and breast (Teoh et al., 2011). One of the reasons why VMAT is easily implemented is that this technology can be adapted to a conventional linear accelerator, just like IMRT. With the increase and versatility in the implementation of this technology, most facilities have upgraded their linacs to deliver VMAT treatments. Early studies of VMAT suggested that this delivery has an increased leakage workload (Teoh et al., 2011) when compared to a conventional open-field delivery technique, similar to IMRT. Simultaneously, with VMAT reducing the overall treatment time, primary weekly workloads have not significantly increased. The overall treatment time that is saved for each patient using arc delivery, is usually offset by treating more patients daily (Saleh et al., 2017). Although no reports have been found in the literature about insufficiency of existing treatment vaults for VMAT delivery, few attempts have been made to analyze the impact that arc therapy has on the various parameters for the design of structural shielding (Teoh et al., 2011).

Relevant recent studies included retrospective analysis of VMAT's primary workload in different centers. Reis, Alves, & Fairbank (2019) suggested that a "VMAT Factor" or "modulation factor" should be introduced to account for radiation incident on secondary barriers. This proposed factor included the effects of increased radiation production, different field collimation, lower beam-on time, and variable dose rate. This factor is analogous to the "IMRT factor" of Report 151 (referred to as *C* earlier), and their calculation was identical. Their VMAT factor was lower than the corresponding IMRT factor would be for the same barrier and same angular direction; however, the difference was not established within statistical certainty. This study also recognized that the treatment site and fractionation could have a substantial impact on the workload distribution (i.e., use factors), but it was not in their scope to quantify this effect (Reis, Alves, & Fairbanks, 2019).

In 2010, a retrospective study was carried out at Memorial Sloan Kettering Cancer Center to analyze the impact on workload of several treatment modalities over a 10-year timeline. Treatment of different anatomical sites yielded significant differences for the use factors in individual treatment vaults, mainly because of the type of treatment applied to particular sites; when all treatment rooms were aggregated, the differences became insignificant (Saleh et al., 2017). Figure 1.1 presents their results on the spatial distribution of the workload, i.e., use factor, shown as a rose plot for each type of treatment. These plots clearly indicate that the spatial distributions of use factors are quite different between VMAT and IMRT. This study indicated that the main reason for this difference is due to each delivery technique catering to specific treatment sites, but no proof of this claim was presented.

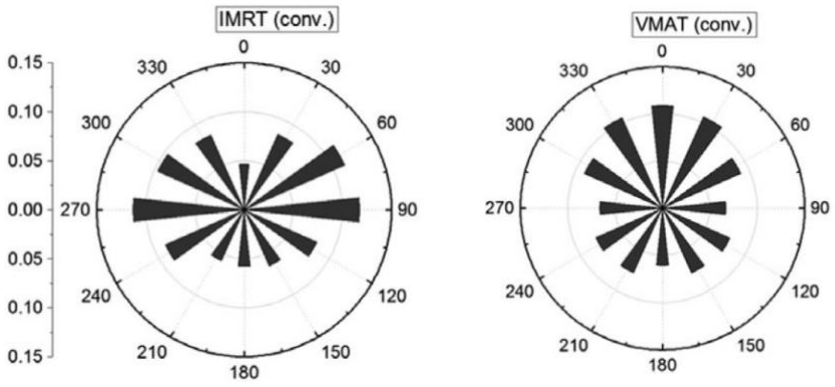

Figure 1.1. Use factors represented as rose plots comparing IMRT and VMAT, aggregated for all treatment vaults over a period of one year. *Source:* Saleh et al., 2017.

1.3. Hypothesis and specific aims

The goal of this project was to assess the impact of VMAT treatment delivery on the design of structural shielding using the methods in Report 151. One aspect was to determine if a vault designed exclusively for VMAT but using only the data available in Report 151, with essentially no additional conservative margin, results in a vault design that would meet design goals. A second

aspect was to identify VMAT-specific issues and to collate VMAT-specific data that could be incorporated into Report 151, ensuring that a vault exclusively designed for VMAT treatments, with minimal conservative margin, would be certain to meet design goals. In other words, is Report 151 as written conservatively safe for VMAT? If not, what additional information or modified methods would render it so?

1.3.1. Hypothesis

The hypothesis for this work is that Report 151, as published, results in a safe shielding design for a dedicated VMAT treatment vault. In other words, the shielding for a linac vault that delivers only VMAT, designed using the methods and supporting data available in Report 151, and incorporating minimal conservative overestimates of parameters, will not exceed design goals for any barrier. The choice of this hypothesis was based on the lack of reports regarding inadequate vaults in the literature.

1.3.2. Specific Aims

1. Collect linac log files for VMAT deliveries from five Elekta linacs at Mary Bird Perkins Cancer Center over 4 months; then catalog the use factors and other patient metrics (workload and modulation) by treatment sites.
2. For a typical vault design, derived from an existing vault used for VMAT, compare barrier calculations based on (a) the use factors determined in Aim 1, (b) the assumption of uniformly distributed use factors, and (c) the IMRT use factors from Report 151. The same minimal conservative margins will be utilized for all cases.

Chapter 2. Data collection methods

This chapter describes the methods used for collection and analysis of linac operation data for VMAT deliveries. Treatment-related metrics were summarized to delineate the "typical weekly workload" for this data; qualified experts can utilize these metrics to assess the results and recommendations of this work relative to their facilities.

2.1. Accelerators and facilities

This VMAT data was collected from five linear accelerators at three facilities operated by the Mary Bird Perkins Cancer Center (MBPCC) in Baton Rouge, in Covington, and in Gonzalez. The five accelerators were all manufactured by Elekta. One linac in Baton Rouge (BR1) was an Agility model while the other (BR2) was a Versa HD model. Both linacs in Covington (CV1 and CV2) and the linac in Gonzalez (GON) were Agility models. The Elekta Versa HD model is an upgrade to the Agility, providing high dose rates for SBRT and SRS treatments; these models have no significant differences in terms of shielding design, however. All linacs are used daily for a mix of VMAT and other types of treatment deliveries.

2.2. Collection of linac operation data

2.2.1. Linac log files

During any radiotherapy delivery, the treatment control system of the linac records the complete machine state at a sampling rate of 4 Hz. After each delivery, this log file is temporarily available for retrieval from the linac (Grenier, 2013). MobiusLog (Mobius Medical System, LP, Houston, TX) is the software package used at MBPCC to retrieve and archive the log file. MobiusLog can record 200-300 control points per delivery; each control point records mechanical parameters such as timestamp, gantry position, monitor units delivered, collimator position, and leaf position data. Each log file is uniquely named so that the data can be associated to the patient's

treatment records. The log file also records the patient ID number, patient name, and the delivery date and time.

Log files were collected by MobiusLog for all treatment deliveries on the five linacs over a 4 month period. MobiusLog writes the log file data into two files, one containing the treatment information (with a '.elog' extension) and the other (with a '.ebin' extension) containing the real time linac mechanical state recorded at the 4 Hz sampling rate. The '.elog' file is written in human-readable format as shown in Figure 2.1, while the '.ebin' file has a human-readable header followed by binary data which must be decoded, as shown in Figure 2.2. All files were anonymized by removing or overwriting patient specific data, and by renaming the files with the date and timestamp only.

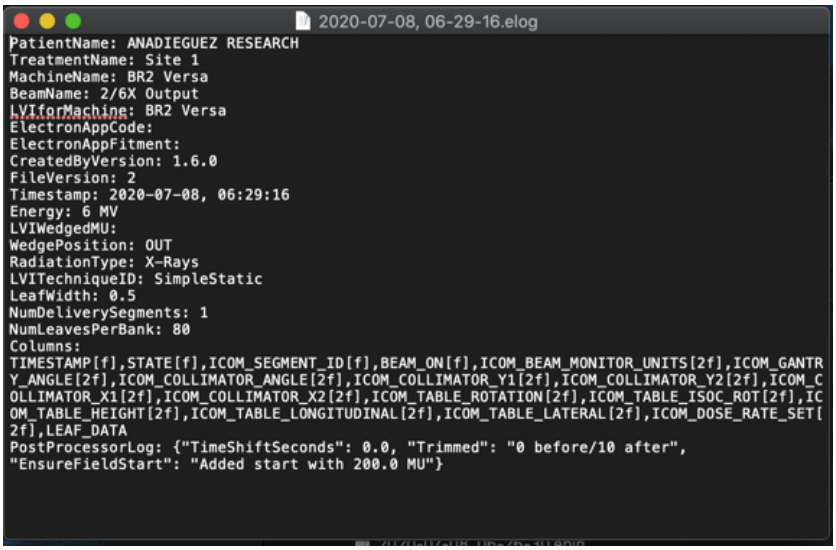

Figure 2.1. Screen capture comparing the contents of an '.elog' file generated by MobiusLog. The '.elog' file only contains a header with information of the treatment set up. i.e. beam name, technique, and delivered Mus The "Columns" row of the header lists the categories of data contained in the '.ebin' file.

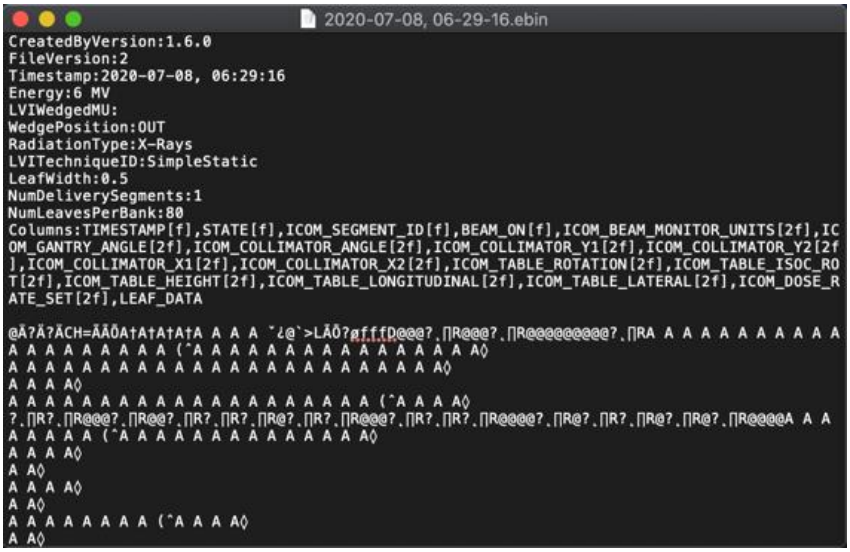

Figure 2.2. Screen capture comparing the contents of an '.ebin' file generated by MobiusLog. This '.ebin' file contains a header with treatment information followed by binary data that needs further decoding and contains the gantry mechanical state at control points and the "Columns" row of the header lists the categories of data contained in the '.ebin' file.

2.2.2. Data parsing from log files

Each '.ebin' file was parsed using an in-house Python Spyder script. The binary portion of an '.ebin' file contained 1400 bytes of information per control point. The first 120 bytes recorded 17 variables describing the radiation beam's position and state, with the data stored in an order indicated in the file header. The pertinent beam information for this project included the control point's timestamp (in milliseconds since the start time of the arc's delivery), position of the gantry, beam state, dose rate, and monitor units delivered. The remaining bytes for each control point contained position of the collimator, couch angular position, whether external beam modulators were used, and state information about the 80 leaves of the multileaf collimator, which were not relevant to this work. The Python script determined the number of control points from the amount of binary data stored in the file, and allocated storage for the data of each control point. The binary data was then read byte by byte as a big-endian single-precision float type. The parsed data was

written into a '.csv' format spreadsheet for subsequent analysis. The timestamp and treatment site were used as the '.csv' file's name.

The treatment site and delivery method (conventional, IMRT, or VMAT) was determined from the headers of the '.ebin' and '.elog' files. The python script contained a set of logical conditions that classified the treatment site based on key words, e.g. sites containing the keywords *prostate* or *prostatic* were classified as *pelvis* for the treatment site. Eight classifications were chosen for treatment sites: *abdomen*, *chest* (treatment to the chest wall), *head & neck*, *lung* (treatment to a tumor within the lung), *pelvis* (most often, treatment of the prostate), *spine*, *QA*, and *other*. Within each type of treatment site, VMAT treatment plans are similar as to how the arcs are planned and delivered. These site classifications were chosen in consultation with clinical medical physicists at MBPCC (D. Neck and J. Fontenot, private communication), representing the majority of VMAT treatments delivered on the five linacs at the three facilities.

A master spreadsheet was developed to associate the '.csv' file with the original '.ebin' file and '.elog' file. The '.elog' file contained information such as the linac name which wasn't in the parsed '.ebin' file, so this global list facilitated crosschecking of information during analysis. The global list was also used to tally numbers and types of treatments on each linac per day, numbers of beams delivered, and additional information that was used to categorize the delivery data, as described in the next section.

A note on terminology in the following sections, a *beam* refers to delivery of radiation to the patient. For VMAT, one delivered arc is a beam; a VMAT treatment on a single day may comprise one, two, or a few arcs. For IMRT, a beam is multiple small (modulated) fields delivered from a single gantry position; an IMRT treatment typically delivers a large number of beams. Finally, a

conventional treatment delivers one or more static (unmodulated) beams from specific gantry positions.

2.3. Arc delivery metrics

Log files for treatment deliveries on the 5 linacs were recorded in the months of September, October, November, and December of 2020. Overall, MobiusLog recorded 23,895 deliveries during this span of 4 months. The number of treatments delivered and to which treatment sites varied from day to day; even though patients come in regularly through each week, fluctuations occur as new cases start and other treatment courses end. The treatment deliveries were catalogued in terms of number of deliveries per treatment site, number of arcs delivered per fraction, prescribed dose, and total arcs delivered per patient. In this study, a five-number summary was used to describe each metric. The five-number summary included the data series' minimum, first quartile, median, third quartile, and maximum; first and third quartiles are often reported together as interquartile range (IQR). The arithmetic mean was also determined; a comparison of mean and median can illustrate asymmetry of the data distributions (Massart, Smeyers-Verbeke, Capron, & Schlesier, 2005). The summary data was used to analyze workload and modulation. The summary data also allows qualified experts to compare the treatment census at their institutions to that reported in this work.

2.3.1. Clinical case metrics

The clinical case metrics over the 4-month period were combined to define a typical daily patient workload for each linac and for all linacs together (all treatment sites combined), as well as for each treatment site (all linacs combined). The typical daily workload characterized the total number of arcs delivered on an average day. As the first step, the occurrences of the different treatment sites across all delivery methods (conventional, IMRT, and VMAT) were determined

from the log file data, shown in Table 2.1. Overall, the most frequently treated site was the pelvis, with a median daily case count of 61, followed by lung with 55, and then head & neck with 41.

Table 2.1. Statistics regarding beam deliveries per treatment site for all linacs and all treatment methods (conventional, IMRT and VMAT). IQR = interquartile range. Figure A.1 shows this data as a boxplot.

Site	**Total beams delivered***	**Beams delivered per day**				
		Min	Mean	Median	IQR	Max
Abdomen	936	3	12.8	14	[10,15]	20
Chest	2594	6	34.1	27	[23,35]	48
H&N	3032	4	35.3	41	[30,35]	65
Lung	3937	14	51.8	55	[43,63]	82
Pelvis	4600	24	59.0	61	[51,75]	110
Spine	1232	2	16.9	14	[10,20]	33
QA	5006	1	54.4	60	[33,72]	124
Others	2558	1	32.4	36	[24,42]	58

*Total number of beams delivered on all 5 linacs over 4-month period

Analyzing only the VMAT deliveries, the most frequently treated sites were still the pelvis, lung, and head & neck (Table 2.2). While VMAT was utilized to some extent for all treatment sites, comparing Table 2.2 to Table 2.1 shows that VMAT was the predominant choice of treatment method for each of these three sites. VMAT was used almost exclusively for treatment of the pelvis (median of 58 VMAT arcs out of 61 beams delivered, or 95%) and head & neck (median of 37 VMAT arcs out of 41 beams delivered, or 90%).

2.3.2. Machine metrics

Table 2.1 and Table 2.2 showed the daily deliveries for each treatment site for all linacs. Because shielding is designed individually for each treatment room, Table 2.3 and Table 2.4

summarize the delivery data by linac for all treatment sites for all delivery methods and for VMAT only, respectively. The data of Table 2.4 is also illustrated in Figure 2.3. These tables illustrate differences in utilization of the linacs at the several MBPCC facilities, including the proportions of VMAT to other delivery methods.

Table 2.2. Statistics regarding VMAT arc deliveries per treatment site for all linacs. IQR = interquartile range. Figure A.2 shows this data as a boxplot.

Site	**Total arcs delivered***	**Arcs delivered per day**				
		Min	Mean	Median	IQR	Max
Abdomen	468	2	6.5	6	[8,12]	12
Chest	395	1	5.4	9	[3,12]	13
Head & Neck	2700	15	32.1	37	[29,42]	51
Lung	3034	14	40.5	39	[34,49]	64
Others	963	1	12.5	12	[8,17]	25
Pelvis	4283	24	55.6	58	[49,70]	89
QA	387	3	20.4	7	[7,27]	49
Spine	176	1	3.7	2	[2,4]	7

*Total number of arcs delivered on all 5 linacs over 4-month period

The two linacs in Baton Rouge were the most used overall; 62% of treatments (a median of 51 of 82 beams per day) on BR2 were VMAT deliveries, but only 38% of treatments on BR1 were VMAT. Because of the model difference between BR1 and BR2, conventional treatments and IMRT are more prevalent on BR1, while BR2 is designed for high dose rate treatment deliveries. The three linacs in Covington and Gonzalez were all similar in utilization, with VMAT accounting for just under half of all treatments on these linacs. From a qualitative assessment of the master spreadsheet, outliers in Figure 2.3 showing heavier and lighter utilization on some linacs likely

indicate isolated days of maintenance procedures on a linac when treatments were shifted to another linac, as well as heavy QA workloads on some linacs.

Table 2.3. Statistics regarding beam deliveries per linac for all treatment methods and sites. IQR = interquartile range. Figure A.3 shows this data as a boxplot.

Machine	**Total beams delivered***	Beams delivered per day				
		Min	Mean	Median	IQR	Max
BR1	5161	2	79.4	91.5	[55.0, 103.0]	169
BR2	6211	32	79.6	82	[65.0, 92.0]	129
CV1	5525	37	72.7	68.5	[62.0, 79.0]	104
CV2	4951	33	71.8	71	[60.5, 80.0]	93
GON	3607	31	63.3	76	[52.0, 76.0]	107

*Total number of arcs delivered on all 5 linacs over 4-month period

Table 2.4. Statistics regarding VMAT arc deliveries per linac for all treatment sites. IQR = interquartile range. Figure 2.6 shows this data as a boxplot.

Machine	**Total arcs delivered***	**Arcs delivered per day**				
		Min	Mean	Median	IQR	Max
BR1	2484	2	38.5	35.0	[24,55.5]	87
BR2	4065	13	52.1	51.0	[43.8,65]	87
CV1	2286	12	30.1	31.0	[26,35.8]	49
CV2	2318	16	33.6	34.0	[28,39.5]	52
GON	1779	16	31.2	32.0	[28,37]	45

*Total number of arcs delivered on all 5 linacs over 4-month period

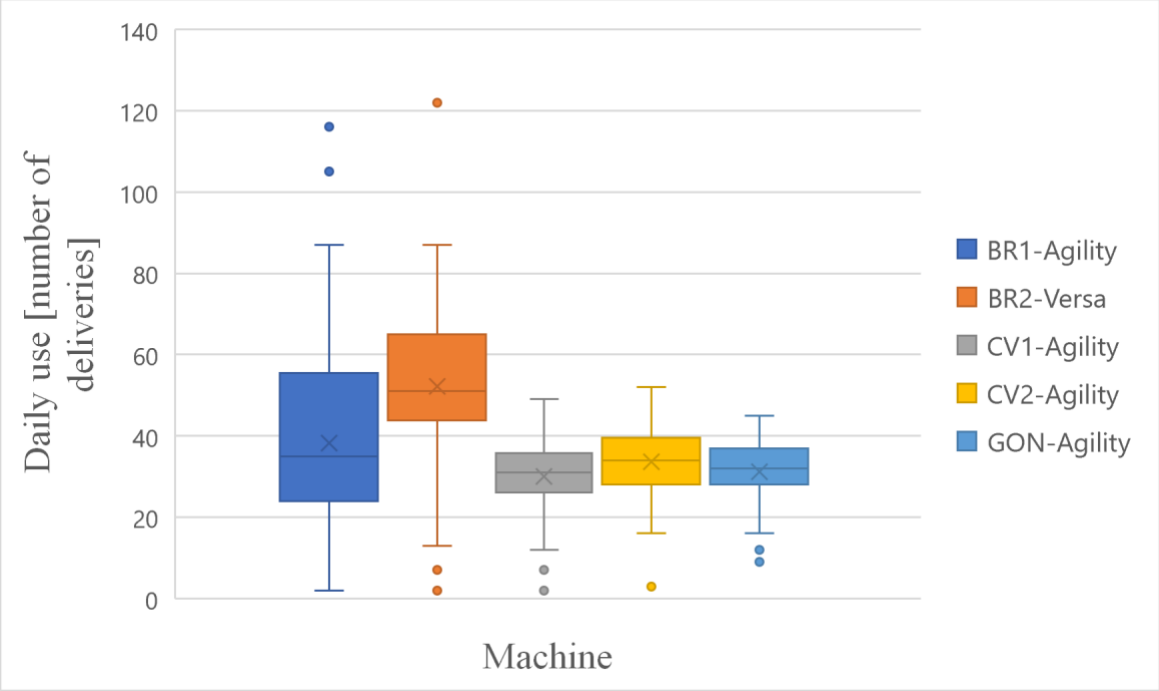

Figure 2.3. Boxplot illustrating linac usage for VMAT deliveries. The box sides represent interquartile range (IQR), which contains 50% of the data points. The line within the IQR shows the median, with the cross indicates the mean. The whiskers mark the minimum and maximum values of the data range, with outliers (circles) defined as points that are more than 1.5 times the IQR from the median value.

2.3.3. Workload and modulation

The log files contain information about the beam output at a given control point, measured in monitor units (MU), and also the cumulative MU delivered. The beam output is measured by the dose monitoring system in the treatment head (Khan, 2014). MU directly measures radiation production by the linac. Beam modulation causes the MU to be larger than the workload, i.e., dose delivered to isocenter; modulation blocks parts of the produced radiation from reaching the patient. Workload can be derived from prescribed dose per fraction and the patient's fractionation scheme. Because prescribed dose is not a mechanical variable, it was not included in the log file for a treatment. Instead, the prescribed dose delivered by each beam and the fractionation scheme was retrieved from MOSAIQ (Elekta AB, Stockholm, Sweden), software used to track patient

information and treatment records. The total workload for each machine was obtained by tallying the dose delivered to all patients over the 4 month period. Filtering the master spreadsheet per month and per machine, the monthly workload per machine was tallied. Then the daily workload per machine can be found based on the number of treatment days in each month. From this, the average daily workload was calculated, as well as an average weekly (assumed 5-day work week) value for each machine (Table 2.5) to be used in shielding calculations.

BR2 had the highest workload for VMAT deliveries, nearly a factor of 2 higher than BR1, but similar to both CV1 and CV2. The primary reason for this higher workload is that all three machines can deliver stereotactic body radiotherapy (SBRT). SBRT treatments deliver large doses per fraction in a hypofractionated regimen (Benedict et al., 2010); an order of magnitude more radiation is delivered per fraction, but still with only a few arcs. SBRT treatments on BR2, CV1, and CV2 result in substantially higher workload, but without a correspondingly larger number of delivered arcs compared to the other linacs.

Table 2.5. Average weekly VMAT workload for each linac for all treatment sites combined. These values were used as W in shielding calculations, e.g., in Eq. 1.

Machine	**Daily workload September [cGy]**	**Daily workload October [cGy]**	**Daily workload November [cGy]**	**Daily workload December [cGy]**	**Workload [Gy/week]**
BR1	16673.8	18709.9	19857.4	13621.3	685.0
BR2	18112.8	11966.6	12536.1	18896.3	944.7
CV1	16120.4	18714.3	19650.0	14019.4	856.3
CV2	15578.7	18732.9	19569.8	11039.4	811.5
GON	15759.3	14999.4	1950.3	13849.3	582.0

Due to VMAT's use of modulated fields to achieve conformality, just like IMRT, shielding calculations require a modulation factor to account for the extra radiation produced by the linac compared to the radiation delivered to the target. Modulation factor was defined by Report 151 as the leakage factor and is calculated with Eq. 4 and Eq. 5 and associated text in Chapter 1. The average dose per arc was calculated from the average workload and the average number of arcs delivered. The average beam output (MU) per arc was determined from the log file data. The average MU for a VMAT delivery was then calculated using Eq. 4. All MBPCC linacs are tuned at installation to have an output factor (MU_{conv}) of 0.8 cGy/MU for an open field at 6 MV, allowing calculation of the modulation factor *C* using Eq. 5. Table 2.6 lists the mean dose per arc, the mean MU per arc, and the resulting mean modulation factor, as well as the median, IQR, min, and max values.

In previous literature, a VMAT modulation factor of 4.6 $\pm$1.6 was reported (Saleh et al., 2017). This reported factor fell within the IQR of this study's data. Report 151 noted that IMRT modulation factors typically fall in the range of 2-10 range (NCRP, 2005), which encompassed the mean value of 3.32 found for VMAT in this work.

Table 2.6. Average modulation factor for VMAT treatments across all five linacs. Figure A.3 shows this data as boxplot.

Mean dose per arc	**Mean MU per arc**	C_{VMAT} **Mean**	C_{VMAT} **Median**	C_{VMAT} **IQR**	**Min**	**Max**
117.4 cGy/arc	331.9 MU/arc	3.32	3.45	[2.60, 4.28]	0.26	6.82

2.4. Summary

The goal of having well-characterized clinical metrics for the MBPCC facilities and linacs was to provide qualified experts with the ability to relate the metrics and results of this project to the particular circumstances of their facilities. All data reported in this chapter, for both individual treatment sites and individual linacs, is presented in Table 2.7. The total workload is based on the classification of each machine's workload presented in Table 2.5 by treatment site; it is a direct summation, not an average value. All average values for daily cases and weekly workloads represent the median of the data set, unless otherwise indicated.

Table 2.7. Summary of metrics per linac and treatment site. All entries are median values.

Site	Machine	BR1 VMAT	BR2 VMAT	CV1 VMAT	CV2 VMAT	GON VMAT	Totals		Typical arcs per treatment
							ALL	VMAT	
Abdominal	Daily beams	1.1	1.6	1.4	1.4	1	14	6	2
	Workload [Gy]	86.9	120.8	108.6	102.9	73.8	--	491.9	
	Weekly work-load [Gy]	9.6	18.5	9.6	8.4	6.7	--	116.4	
Chest	Daily beams	7.5	10.3	9.3	8.8	6.3	39	27	2
	Workload [Gy]	390.8	539.0	488.5	463.0	332.0	--	2213.3	
	Weekly work-load [Gy]	92.5	127.5	115.6	109.6	78.6	--	756.5	
Head & Neck	Daily beams	7.1	9.8	8.9	8.4	6.0	41	37	2
	Workload [Gy]	535.6	738.6	669.5	634.5	455.0	--	3033.1	
	Weekly work-load [Gy]	126.7	174.8	158.4	150.1	107.7	--	717.7	
Lung	Daily beams	7.5	10.3	9.3	8.8	6.3	55	39	2
	Workload [Gy]	564.5	778.5	705.7	668.7	479.6	--	3394.8	
	Weekly work-load [Gy]	133.6	184.2	167.0	158.2	113.5	--	212.1	

(table cont'd)

	Machine / Site	BR1 VMAT	BR2 VMAT	CV1 VMAT	CV2 VMAT	GON VMAT	Total ALL	Total VMAT	Typical arcs per treatment
Pelvis	Daily beams	11.1	15.3	13.9	13.1	9.4	61	58	2
	Workload [Gy]	839.5	1157.8	1049.5	994.5	713.3	--	501.1	
	Weekly work-load [Gy]	198.7	274.0	248.3	235.3	168.8	--	31.3	
Spinal	Daily beams	0.4	0.5	0.5	0.5	0.3	14	2	2
	Workload [Gy]	28.9	39.9	36.2	34.3	24.6	--	4789.6	
	Weekly work-load [Gy]	6.9	9.4	8.6	8.1	5.8	--	299.4	
QA	Daily beams	1.3	1.8	1.7	1.6	1.1	60	7	1
	Workload [Gy]	101.3	139.7	126.7	120.0	86.1	--	--	
	Weekly work-load [Gy]	24.0	33.1	30.0	28.4	20.4	--	--	
Others	Daily beams	2.3	3.2	2.9	2.7	2.0	36	12	2
	Workload [Gy]	173.7	239.5	217.1	205.8	147.6	--		
	Weekly work-load [Gy]	41.1	56.7	51.4	48.7	34.9	--	24.2	
Total	Daily beams	21.5	63.5	36.1	31.9	26.1	308	200	
	Workload [Gy]	2,722.9	5,294.7	5,294.7	2,420.4	1,966.4	--	15,127.4	
	Weekly work-load [Gy]	685.0	944.7	856.3	811.5	582.0	--	3,579.5	

Chapter 3. VMAT use factors

This chapter presents methods and results for extracting use factors from the VMAT log files; the use factors were quantified and compared over several angular binning intervals. These intervals included the 45° and 90° intervals used in Report 151 as well as smaller intervals of 15° and 30°. Use factors were examined both as composite values combining all treatment sites and as treatment site-specific values. Results were compared to the recommended use factors from Report 151 and to the assumption of uniform gantry rotation. Chapter 4 provides sample shielding calculations that compare the impact of the various use factor results.

3.1. Methods

NCRP Report 151 defines the use factor as "the fraction of the weekly workload for which the gantry or beam is oriented in [a specified] angular interval centered about [a specified] angle" (NCRP, 2005). To determine a use factor, one first specifies the desired range of gantry positions, typically as an angular interval centered at a particular position; one then sums the workloads delivered at each gantry position within the range, and normalizes to the total workload. Report 151 notes that the characteristics of a treatment technique, such as total body irradiation and IMRT, can significantly impact the use factors, and admonishes qualified experts to assess this as part of shielding design. VMAT-specific use factors were extracted from the data in each ".ebin" log file. Each entry for a control point recorded the gantry position; therefore, each control point was easily assigned to a use factor interval. The total number of control points over which the beam delivers radiation was used to normalize the number of control points in each interval. The MBPCC linacs were configured to report gantry positions over the range of -180° to +180°, with the 0º position referring to the gantry pointing downwards (radiation beam directed towards the floor); a positive change in angle represented a clockwise gantry rotation, as one faces the gantry across isocenter.

In contrast, Report 151 defines use factors over the range of 0° to 360º. Therefore, each gantry position G reported in the VMAT log files was transformed as $(G + 360)\ modulo\ 360$, to match the convention of Report 151. A Python script was used to classify all control points into the interval ranges of the desired binning scheme. Four binning schemes were assessed: 90º, 45º, 30º, and 15º ranges with evenly spaced bins, with the first bin centered at G=0º (*i.e.* the gantry pointing down). Once the gantry position data was classified into the bins, a frequency analysis (i.e., normalization to the total number of control points) was done for each bin to obtain the use factor. The next section presents the VMAT use factors for the four binning schemes, followed by a section comparing these results to the recommended use factors at 90° and 45° intervals of Report 151. The final section discusses variations in the VMAT use factors between treatment sites.

3.2. VMAT use factors vs. binning scheme

Figure 3.1 compares the VMAT use factors for the four binning schemes: 90º, 45º, 30º, and 15°. These use factors are composite values for all linacs and all treatment sites. In these plots, the labels are placed at the corresponding position of the gantry head, e.g., 0º represents the gantry head located above the patient and pointing towards the floor while 180° is the gantry head at the floor directed up toward the ceiling. Therefore, the wedge located under the 0° label reports the use factor for the section of floor below isocenter when the gantry is positioned at 0°. In each binning scheme, the VMAT use factor for the interval centered at 180º (beam pointed towards the ceiling) was consistently the smallest; to avoid mechanical collision and allow clearance around the treatment couch, VMAT plans rarely pass through the 180° gantry position. Similarly, the use factor at 0° was consistently larger than the rest. VMAT arcs are typically larger than 180° in span, so essentially every arc passes through the 0° gantry position.

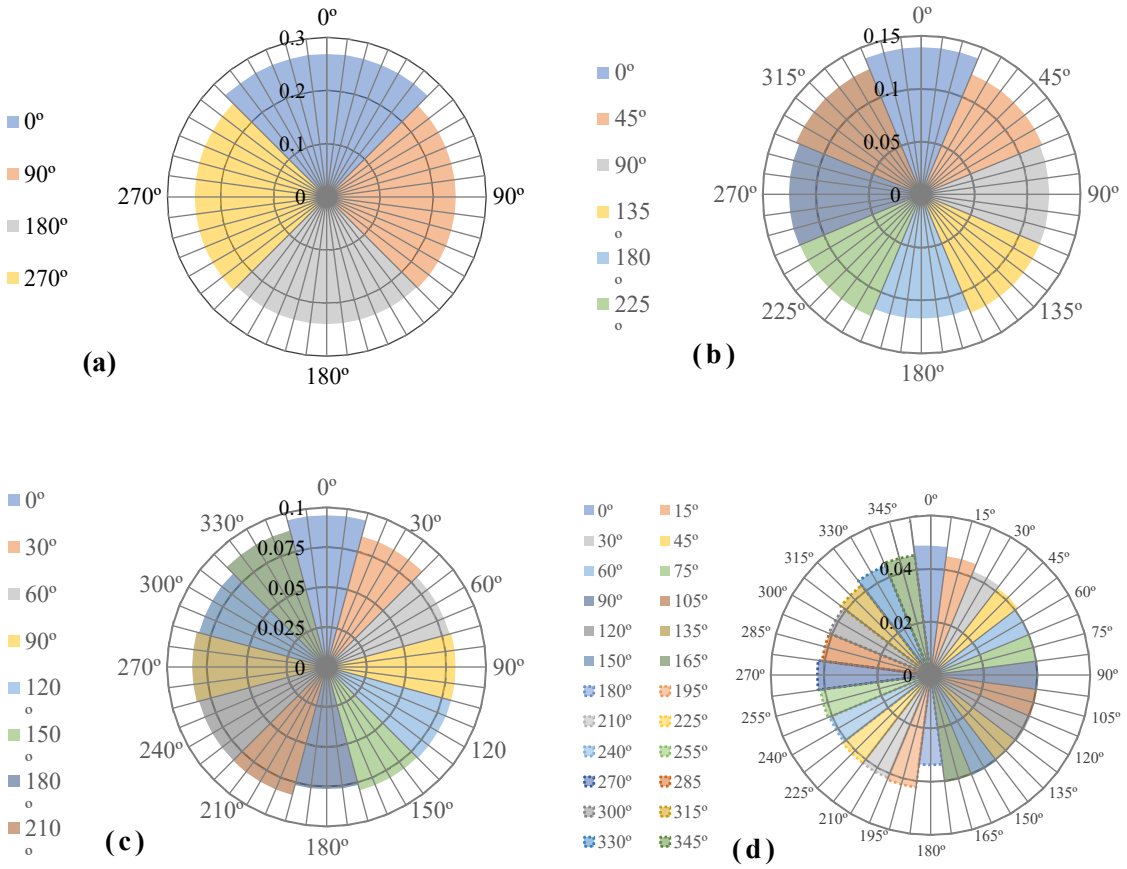

Figure 3.1. VMAT use factors for all treatment sites and all linacs, for the four binning schemes: (a) 90°, (b) 45°, (c) 30°, and (d) 15° intervals. The first interval is always centered on 0°; this wedge represents the use factor for the floor directly beneath isocenter.

Table 3.1 reports numerical values for the use factors shown in Figure 3.1. The reported uncertainties were calculated by averaging the use factors determined for each month of log files. These uncertainties were only intended to qualitatively gauge the variability over time of the use factors. Appendix B.2 provides mean, median and IQR results and corresponding box plots, as an alternative representation to the radar plots of Figure 3.1 and Table 3.1.

The coarse 90º interval use factors averaged out much of the small variations that were visible at the finer binning schemes, especially the 15° interval. The use factors appear to scale between binning schemes essentially as the ratio of the interval sizes, so using a finer binning scheme results

in a larger barrier transmission and correspondingly thinner barrier than a coarser scheme. However, the finer binning schemes, especially the 15° interval, would likely be the most susceptible to variations in use factors due to changes in utilization (overall number of VMAT treatments or numbers of deliveries to specific treatment sites). While potentially yielding a short-term savings in materials and cost, using too fine of a binning scheme could result in inadequate barriers. A viable option would be to use the 45º or 30º interval use factors for wall and floor calculations to minimize materials, space, and cost; the 30° or even 15° interval use factors would be useful for designing a tapered ceiling barrier. These issues are discussed further with the sample shielding calculations in Chapter 4.

3.3. VMAT use factors compared to Report 151

The 90º and 45º interval binning schemes for use factors allow specific comparison to the recommended 90° (conventional) and 45° (IMRT) use factors in Report 151. Figure 3.2, Figure 3.3, and Table 3.2 provide this comparison. The uncertainties listed in Table 3.2 again represent the standard deviation of monthly variations. Overall, the 90º interval VMAT use factors were similar to Report 151's 90º interval use factors, since for conventional treatments each of the four directions are about equally weighted.

Table 3.1. Summary of the VMAT use factors derived for binning schemes with intervals of 90º, 45º, 30º, and 15°.

90º interval		**45º interval**		**30º interval**		**15º interval**	
0º	0.271 ± 0.034	0º	0.141 ± 0.018	0º	0.096 ± 0.004	0º	0.050 ± 0.002
90º	0.248 ± 0.019	45º	0.127 ± 0.010	30º	0.087 ± 0.004	15º	0.048 ± 0.002
180º	0.240 ± 0.021	90º	0.124 ± 0.011	60º	0.083 ± 0.003	30º	0.045 ± 0.002
270º	0.242 ± 0.025	135º	0.124 ± 0.015	90º	0.084 ± 0.003	45º	0.044 ± 0.001
		180º	0.117 ± 0.010	120º	0.084 ± 0.003	60º	0.042 ± 0.001
		225º	0.121 ± 0.014	150º	0.083 ± 0.004	75º	0.042 ± 0.001
		270º	0.121 ± 0.014	180º	0.078 ± 0.003	90º	0.043 ± 0.002
		315º	0.125 ± 0.013	210º	0.082 ± 0.003	105º	0.043 ± 0.001
				240º	0.081 ± 0.003	120º	0.043 ± 0.002
				270º	0.082 ± 0.004	135º	0.042 ± 0.002
				300º	0.081 ± 0.003	150º	0.043 ± 0.002
				330º	0.088 ± 0.005	165º	0.043 ± 0.002
						180º	0.035 ± 0.001
						195º	0.043 ± 0.002
						210º	0.041 ± 0.002
						225º	0.041 ± 0.002
						240º	0.041 ± 0.002
						255º	0.041 ± 0.002
						270º	0.042 ± 0.002
						285º	0.040 ± 0.002
						300º	0.040 ± 0.001
						315º	0.041 ± 0.002
						330º	0.044 ± 0.003
						345º	0.046 ± 0.002

Table 3.2. Comparison of VMAT use factors to recommended Report 151 use factors for 90º and 45° binning intervals.

	Bin	VMAT use factor	Report 151 use factor
90° intervals	0º	0.271 ±0.007	0.310
	90º	0.248 ±0.019	0.213
	180º	0.240 ±0.005	0.263
	270º	0.242 ±0.023	0.213
45° intervals	0º	0.141 ±0.006	0.256
	45º	0.127 ±0.011	0.058
	90º	0.124 ±0.010	0.159
	135º	0.124 ±0.009	0.04
	180º	0.117 ±0.003	0.23
	225º	0.121 ±0.012	0.04
	270º	0.121 ±0.013	0.159
	315º	0.125 ±0.011	0.058

More substantial differences are apparent when comparing the use factors at the 45º binning intervals. Not surprisingly because of the arc delivery style, the VMAT use factors are closer to uniformly distributed; the Report 151 use factors are noticeably smaller in the diagonal directions, likely due to a predilection of IMRT treatment planners to favor the four cardinal directions. However, as IMRT treatment planning algorithms have evolved, and especially became automated for optimization, more complex IMRT treatments with more beams per treatment and routinely utilizing more gantry positions have developed, such as illustrated in Figure 1.1 (Saleh et al., 2017); the 45° interval use factors in Report 151 may themselves be out of date. One should NOT

use the Report 151 45° interval use factors when designing shielding for vaults that will be heavily used for VMAT.

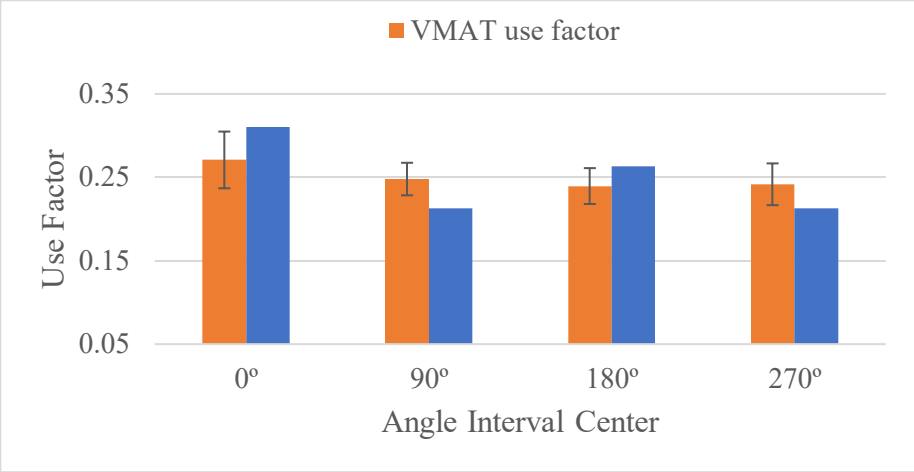

Figure 3.2. Comparison of the 90°-interval use factors from Report 151 vs. VMAT. The error bars represent standard deviation across monthly averages. A fully uniform distribution would have a use factor of 0.25 for each interval.

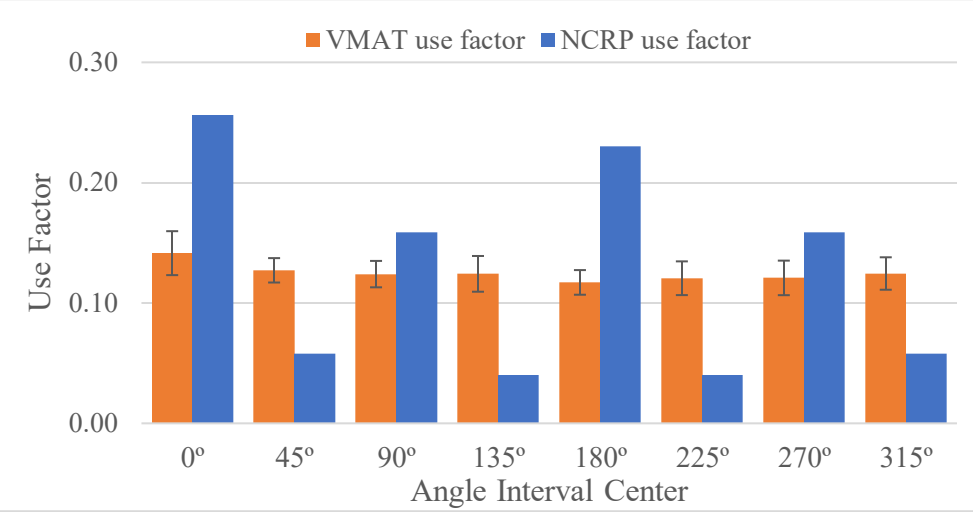

Figure 3.3. Comparison of the 45°-interval use factors from Report 151 vs. VMAT. The error bars represent standard deviation across monthly averages. A fully uniform distribution would have a use factor of 0.125 for each interval.

Overall, the VMAT use factors on 45° intervals were relatively uniformly distributed over the binning intervals. This is not particularly surprising for the VMAT delivery style of large

continuous arcs. The floor and ceiling showed the highest and lowest use factors, respectively, which agreed with the study by Saleh, et.al (Saleh et al., 2017) as shown in Figure 3.4. Saleh's work also showed smaller use factors at 90° and 270°, which were not observed in the current work. The discrepancy may be due to differences in the number of VMAT deliveries to a particular treatment site (see Section 3.4); insufficient detail about the treatment census in the Saleh work limits further discussion of these observed differences.

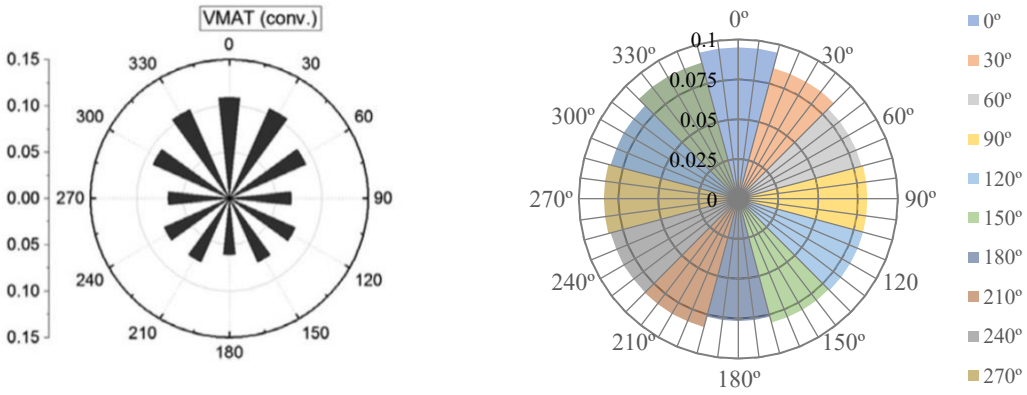

Figure 3.4. Comparison of VMAT use factor distribution with an angle interval of 30º. The rose plot (left) shows the use factors results from previous literature (*Source: Saleh, et.al, 2017*) compared to the radar plot (right) of this study.

3.4. Use factors by treatment site

Based on the comparison in the preceding section between the Report 151 45° interval use factors and the VMAT 45° interval use factors of this work, one might be tempted to say that the VMAT use factors simply represent a uniform distribution of gantry positions. While the results do indicate a relatively uniform distribution, one must keep in mind that those results are a composite of VMAT deliveries to various treatment sites, each with particular treatment goals and organs at risk. Different treatment sites may have unique sets of use factors, as assessed in this

section. Careful consideration must be made by the qualified expert to decide whether the use of site-specific vs. generalized use factors are warranted. Report 151 notes:

> "Clearly, when viewed in 90 degree bins these data [use factors] agree with the expected traditional "four field" approach to treatment. However, upon closer inspection, some of the features that may be unique to a facility begin to appear. For example, a large fraction of tangential breast fields would significantly affect the use factor for gantry angles toward the wall-floor and wall-ceiling interfaces. It is very important that these be considered, especially if any tapering of the barrier thickness is used to account for the beam obliquity."

Studies previous to this work also indicated the need to consider use factors based on the treatment site (Reis et al., 2019). Figure 3.5 shows radar plots of the results of this work's analysis of the use factors based on individual treatment sites. Figure 3.6 shows the same data as overlapping line graphs to facilitate comparison.

Most of the treatment sites followed a relatively uniform distribution of use factors; the two exceptions are chest and lung as evident in Figure 3.6. The chest use factors show strong asymmetry in the anterior-posterior directions. Anatomically, for treatments of the chest, beams are positioned to avoid posterior incidence (i.e the back of the patient) with the patient treated in a supine position; the location of the treated volume is usually anterior with respect to the patient, such as chest wall and breast. Together these factors strongly bias the chest use factors to arcs that move around the anterior of the patient. For the lung, substantial asymmetry is apparent in the left-right directions. This is because lung treatment plans try to spare the contralateral lung as much as possible, so the deliveries are relatively one-sided. (It also appears that the treatment planners may routinely reverse the orientation of right- vs. left-lung patients on the treatment table, rather than reversing which side of the gantry is used to deliver the arcs.)

Figure 3.7 compares the composite use factors to the chest-specific use factors, for 45° intervals. The deviation of chest use factors from the composite use factors is quite noticeable, with the composite values underestimating the chest values for some ranges of gantry motion and

overestimating for the rest. In a linac vault that delivers treatments to a mix of sites, the composite values would be appropriate to use; but if a vault were to be used heavily (or exclusively) for chest treatments, the qualified expert would be wise to use the appropriate site-specific use factors. One can make a similar argument for the lung use factors. This issue is addressed further in the sample calculations in Chapter 4.

In summary, one sees that VMAT use factors generally follow a trend of relatively uniform rotation, if the linac delivers radiation to a variety of treatment sites. With reasonable conservative margins on shielding calculations, both the VMAT use factors presented here vs. use factors based on assumed uniform rotation should yield satisfactory vault designs. However, one should *not* use the 45° interval use factors from Report 151 when designing a VMAT vault. Likewise, if a particular treatment site will dominate the VMAT deliveries in a vault, the qualified expert should consider using treatment site-specific use factors. Sample calculations to illustrate these recommendations are provided in Chapter 4.

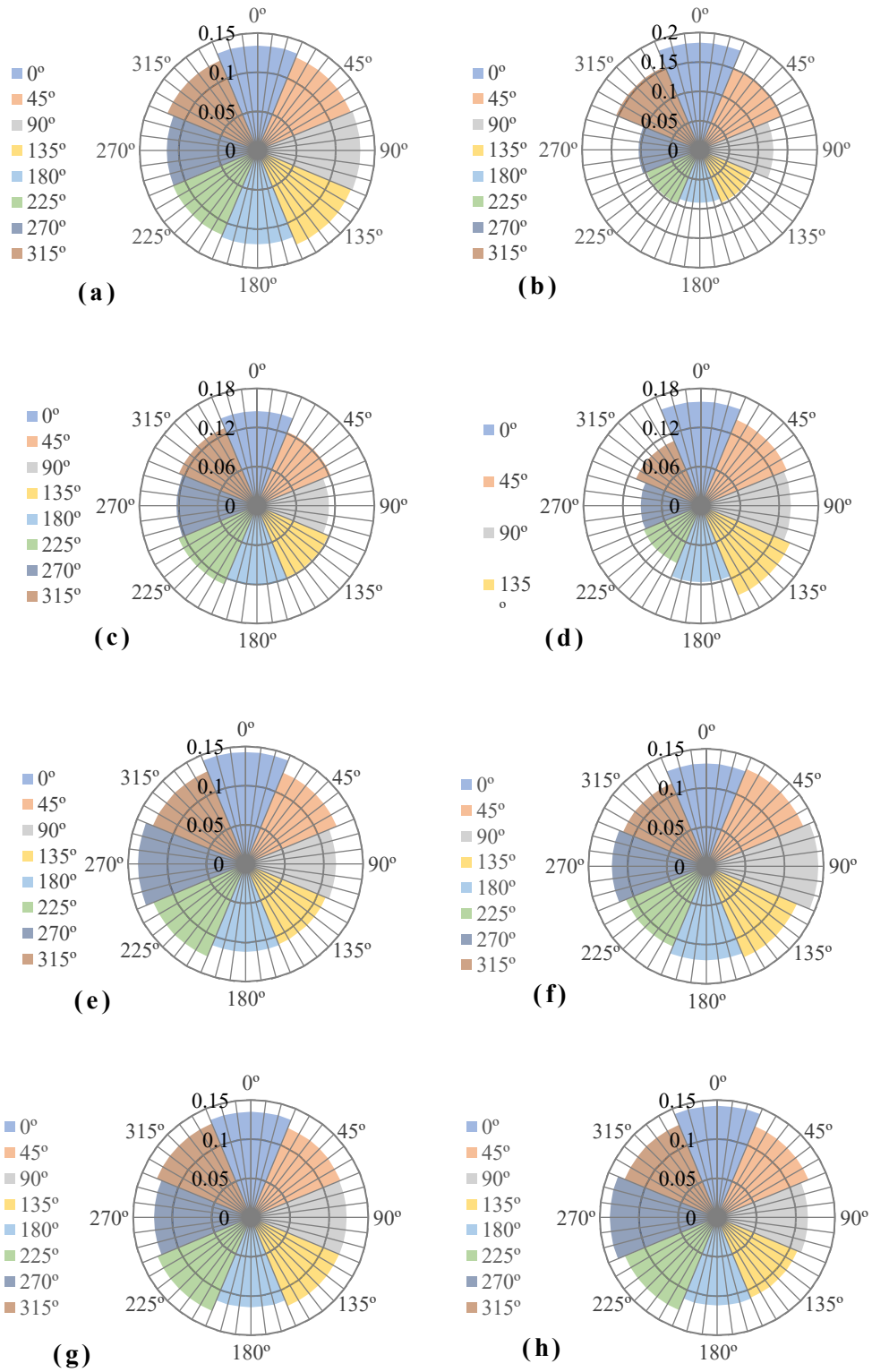

Figure 3.5. VMAT use factors for 45º interval for each treatment site: (a) abdomen, (b) chest, (c) head & neck, (d) lung, (e) pelvis, (f) spine, (g) QA, and (h) others.

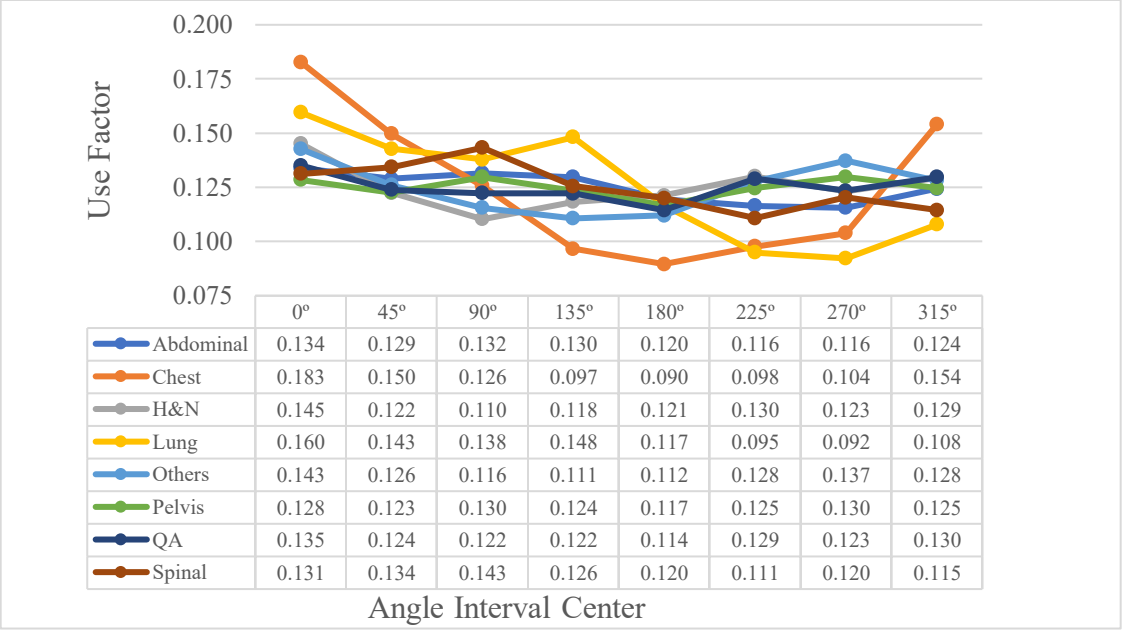

	0º	45º	90º	135º	180º	225º	270º	315º
Abdominal	0.134	0.129	0.132	0.130	0.120	0.116	0.116	0.124
Chest	0.183	0.150	0.126	0.097	0.090	0.098	0.104	0.154
H&N	0.145	0.122	0.110	0.118	0.121	0.130	0.123	0.129
Lung	0.160	0.143	0.138	0.148	0.117	0.095	0.092	0.108
Others	0.143	0.126	0.116	0.111	0.112	0.128	0.137	0.128
Pelvis	0.128	0.123	0.130	0.124	0.117	0.125	0.130	0.125
QA	0.135	0.124	0.122	0.122	0.114	0.129	0.123	0.130
Spinal	0.131	0.134	0.143	0.126	0.120	0.111	0.120	0.115

Figure 3.6. VMAT use factors at 45º intervals for each treatment site. This is the same data as shown in the radar plots of Figure 3.6, but shown as overlays for easier comparison.

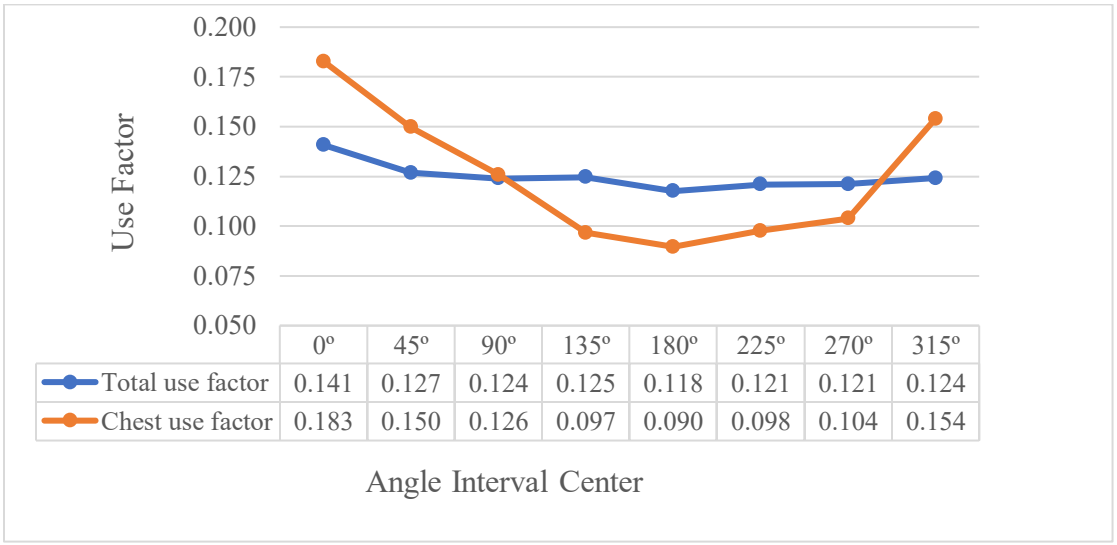

	0º	45º	90º	135º	180º	225º	270º	315º
Total use factor	0.141	0.127	0.124	0.125	0.118	0.121	0.121	0.124
Chest use factor	0.183	0.150	0.126	0.097	0.090	0.098	0.104	0.154

Figure 3.7. VMAT use factors at 45º intervals for the chest treatment side vs. the composite of all treatment sites. The composite use factors underestimathe chest use factors around the 0° gantry position.

Chapter 4. Sample calculations

In this chapter, sample calculations were used to illustrate the impact of VMAT on shielding design. A sample vault layout was created, with the types of areas beyond the barriers chosen to represent typical design goals and occupancies that might be encountered. The sample vault was modeled after the vault that contains the GON linac at Mary Bird Perkins Cancer Center in Gonzalez (D. Neck, private communication). Calculations were performed with realistic geometries, assuming a VMAT-only utilization of the vault, and with minimal amounts of conservative overestimates, to yield fair comparisons. Comparisons were made for the VMAT use factors (combining all sites and all linacs) to the Report 151 recommendations, and also to use factors derived by assuming uniform gantry rotation. The potential impact of treatment site-specific use factors was also assessed. Barriers were designed with the VMAT use factors to just meet the design goals; these were then compared to barriers designed with the other choices for use factors, with all other variables held constant. In all calculations, the VMAT workload determined for the BR2 linac (see Table 2.5) was used, simply because it was the largest workload of the five linacs.

Barrier thickness (t) based on VMAT use factors, Report 151 use factors, or assumed uniform use factors was calculated using Equations 1-7. For additional comparison, the dose equivalent ($H_{shielded}$) beyond the barrier as designed from either the Report 151 use factors or the assumed uniform rotation use factors, but using the VMAT use factors (i.e., assuming the VMAT use factors are the true amount of radiation incident on the barrier), were calculated. An adequate barrier must satisfy:

$$P \geq \mathrm{H_{shielded}} \qquad \text{(Eq. 8)}$$

$$H_{shielded} = H_{unshielded} B_{barrier}$$

The primary unshielded dose equivalent ($H_{unshielded}$) was derived from Eq. 1 (essentially, replacing the design goal P with $H_{unshielded}$ and rearranging). The transmission factor ($B_{barrier}$) for an existing barrier of thickness t is:

$$B_{barrier} = 10^{-\left\{1+\frac{t-TVL_1}{TVL_e}\right\}} \quad \text{(Eq. 9)}$$

All barriers were designed for standard weight concrete, at a beam energy of 6 MV.

4.1. Sample vault design

The sample vault is presented in Figure 4.1. The areas adjacent to the barriers were chosen to highlight a realistic scenario for shielding design. The design parameters are summarized in Table 4.1. Overall vault dimensions and isocenter placement were taken from the design drawings of the vault that inspired this layout. AutoCAD LT (Autodesk Inc, USA) was used to determine distances from isocenter to the points of protection located 30 cm past the barriers (NCRP, 2005). The weekly workload was 960 Gy/week, based on the VMAT workload of the BR2 linac (Table 2.5).

Table 4.1. Shielding parameters for the areas beyond barriers A, C, F and CE.

Barrier	Adjacent area	Occupancy [T]	Design goal [μSv/week]	Distance from isocenter [m]
A (wall)	Uncontrolled waiting area	1	20	6.15
C (wall)	Controlled hallway	1	100	3.34
F (floor)	Controlled laboratory	1	100	1.67
CE (ceiling)	Uncontrolled attic	0.05	20	2.52

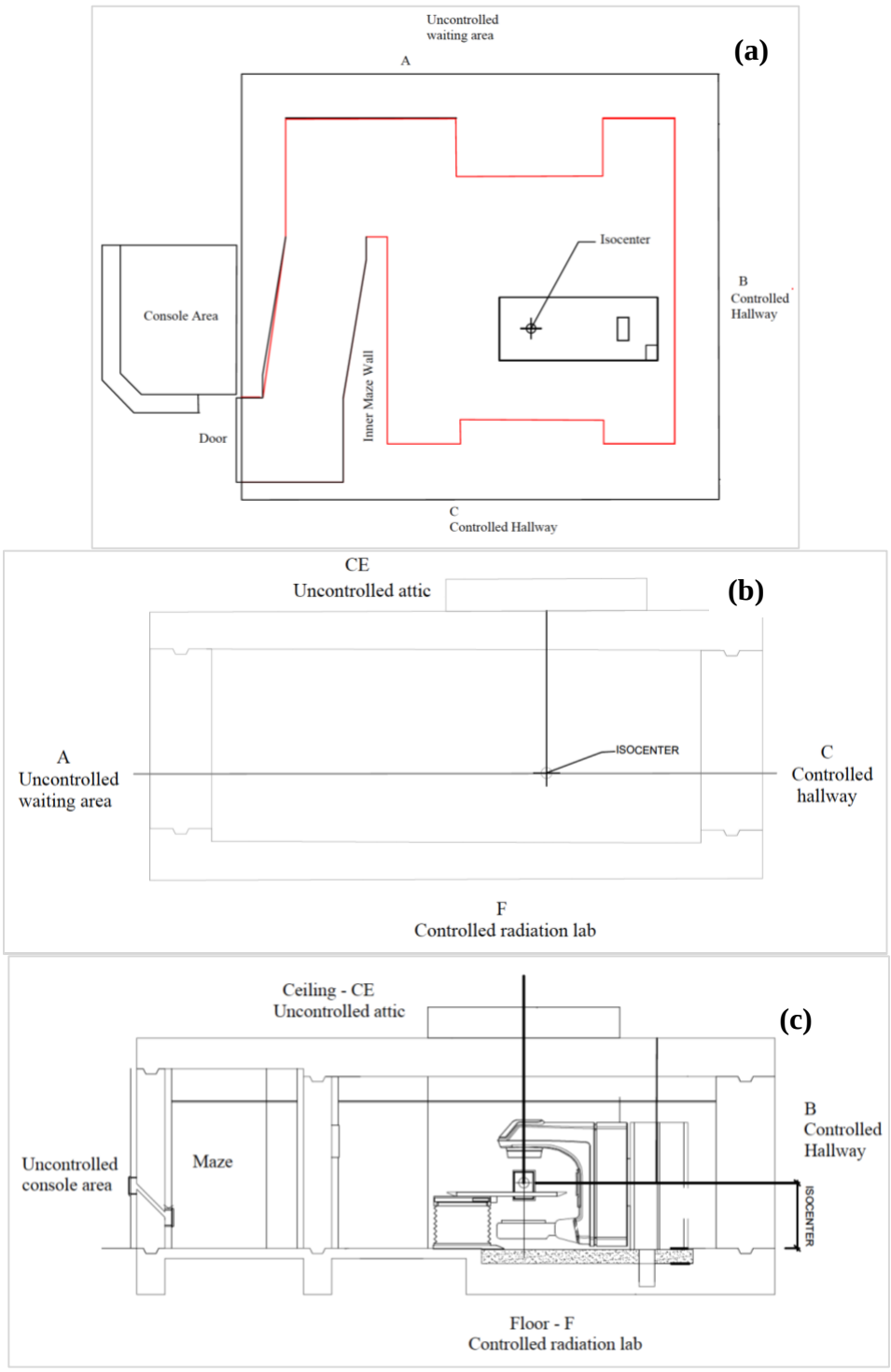

Figure 4.1. Sample vault floor plan. (a) Top view, (b) front elevation through isocenter in the gantry's plane of rotation, and (c) side elevation through isocenter. This floor plan was based on an existing vault at MBPCC (D. Neck, private communication).

4.2. Sample calculations

4.2.1. Shielding design: VMAT vs. Report 151

Report 151 presents two sets of recommendations for use factors: use factors for 90º intervals called “conventional” and for 45º intervals called “IMRT”. The 90º use factors are centered on 0º, 90º, 180º, and 270º gantry positions; the 45° use factors follow the same convention but with centers at multiples of 45º. Figure 4.2 depicts the centers of the intervals, showing how each corresponds to a particular barrier.

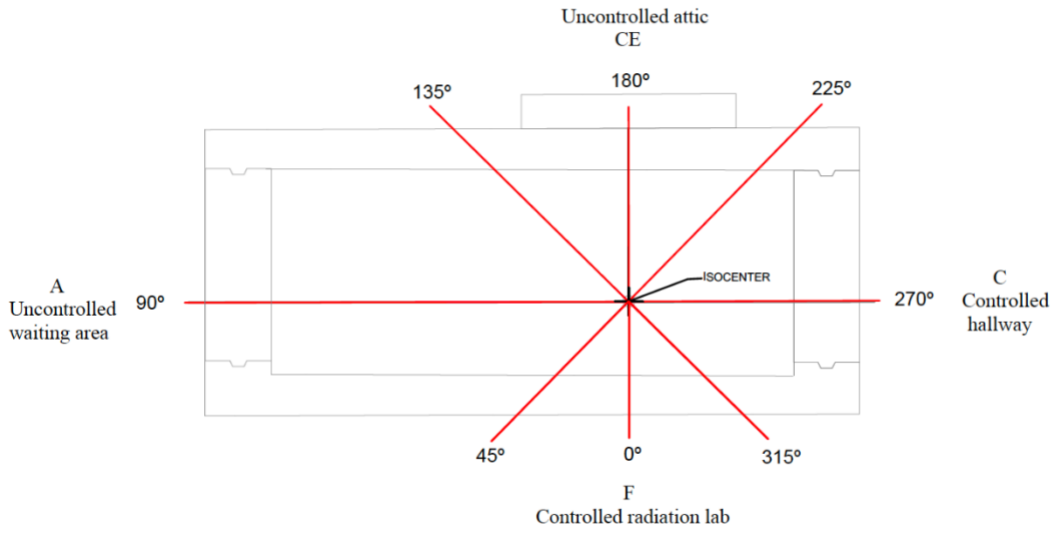

Figure 4.2. Front elevation view through isocenter of the sample vault layout. The red lines represent the centers of the use factor intervals.

Table 4.2 summarizes the barrier thicknesses that result from using the 90° use factors for VMAT vs. Report 151. Also listed are the $H_{shielded}$ values that would result if the Report 151-based barrier thickness must protect from the amount of radiation dictated by the VMAT use factor. Because the VMAT use factors were larger than the Report 151 use factors for the 90° and 270° gantry positions, these barriers (wall A and wall C) if designed with recommended Report 151 use

factors would provide inadequate protection from the actual amount of VMAT workload. By comparison, the floor and ceiling barriers would be adequate. For the walls, small conservative assumptions by the qualified expert such as rounding the barrier thickness to the next inch or overestimating the workload (e.g, using 1000 Gy/week instead of 960 Gy/week) would be sufficient to achieve an adequate barrier when using the recommended 90° use factors from Report 151.

Table 4.2. Comparison of barrier thicknesses when using 90º interval use factors for VMAT vs. Report 151. $H_{shielded}$ is the dose equivalent beyond the barrier when radiation in the amount dictated by the VMAT use factor is incident on the barrier thickness calculated from the Report 151 use factors.

Barrier	VMAT		Report 151		P [μSv/week]	$H_{shielded}$ [Sv/week]
	Use Factor	Thickness [cm]	Use Factor	Thickness [cm]		
A-90º	0.248	181	0.213	178	20	22.9
C-270º	0.242	148	0.213	146	100	107.4
CE-180º	0.240	156	0.263	158	20	16.9
F-0º	0.271	208	0.310	210	100	95.9

Table 4.3 summarizes the barrier thicknesses that result from using the 45° use factors for VMAT vs. Report 151, as well as the $H_{shielded}$ values that would result if the Report 151-based barrier thickness must protect from the amount of radiation dictated by the VMAT use factor. One immediately sees that the barrier thicknesses based on Report 151 use factors in the cardinal directions were satisfactory, but the oblique directions were not. The more uniform distribution of use factors for VMAT means that the Report 151 use factors underestimate the barrier requirements in these oblique directions. Cardinal rather than oblique directions typically dictate wall thickness, so this should not be a concern for the walls. However, a tapered ceiling based on

Report 151 use factors could be inadequate in these oblique directions despite also having longer slanted path lengths. The 45° use factors from Report 151 appear to be adequate for wall barriers, but should not be used if one implements a tapered ceiling barrier.

Table 4.3. Comparison of barrier thicknesses when using 45º interval use factors for VMAT vs. Report 151. $H_{shielded}$ is the dose equivalent beyond the barrier when radiation in the amount dictated by the VMAT use factor is incident on the barrier thickness calculated from the Report 151 use factors.

Barrier	VMAT		Report 151		P [μSv/week]	$H_{shielded}$ [μSv/week]
	Use Factor	Thickness [cm]	Use Factor	Thickness [cm]		
A-45º	0.127	120	0.058	112	20	44.4
A-90º	0.124	171	0.159	174	20	15.1
A-135º	0.124	121	0.040	109	20	59.3
C-225º	0.121	95	0.040	83	100	280.9
C-270º	0.121	138	0.159	142	100	71.0
C-315º	0.125	97	0.058	89	100	201.2
CE-135º	0.124	99	0.040	87	20	58.3
CE-180º	0.117	146	0.230	156	20	9.5
CE-225º	0.121	98	0.040	87	20	57.6
F-45º	0.127	108	0.058	100	100	214.7
F-0º	0.141	168	0.256	176	100	52.4
F-315º	0.125	112	0.058	105	100	202.1

4.2.2. Shielding design: VMAT vs. uniform-rotation use factors

Because the logfile-based VMAT use factors exhibited a relatively uniform distribution, a qualified expert could conceivably choose to approximate the use factors by assuming uniform rotation of the gantry. Table 4.4 compares barrier thickness based on VMAT use factors for 45° intervals to those based on a constant use factor of 0.125 for each interval from assuming uniform

gantry rotation. While some small differences are seen between the VMAT use factors and the constant value of 0.125, simple conservative approaches such as rounding barrier thicknesses to the next cm should be sufficient to compensate. No barriers were substantially inadequate. Therefore, using a constant use factor for 45º intervals appeared to be a safe and adequate approach to barrier design.

Table 4.4. Comparison of barrier thicknesses when using 45º interval use factors for VMAT vs. uniform distribution. $H_{shielded}$ is the dose equivalent beyond the barrier when radiation in the amount dictated by the VMAT use factor is incident on the barrier thickness calculated from the uniformly distributed use factors.

Barrier	VMAT		Uniform		P $\left[\frac{\mu Sv}{week}\right]$	$H_{shielded}$ $\left[\frac{\mu Sv}{week}\right]$
	Use Factor	Thickness [cm]	Use Factor	Thickness [cm]		
A-45º	0.127	120	0.125	120	20	20.1
A-90º	0.124	171	0.125	171	20	19.8
A-135º	0.124	121	0.125	121	20	19.8
C-225º	0.121	95	0.125	95	100	92.1
C-270º	0.121	138	0.125	138	100	93.9
C-315º	0.125	96	0.125	96	100	100

A linac vault's ceiling may need special attention for shielding design, specifically because weight restrictions may make it necessary to take advantage of longer oblique pathlengths by the beam through parts of the ceiling. The more segments that are included in a tapered ceiling, the more savings that occur in weight, so a tapered ceiling barrier was analyzed for use factors on 30º angular intervals to allow for barrier tapering. Like Figure 4.2, Figure 4.3 shows a front elevation view of the sample vault, in this case with red lines marking the centers of the 30º intervals for use factors. The results of the tapered ceiling calculations are shown in Table 4.5 and Figure 4.4.

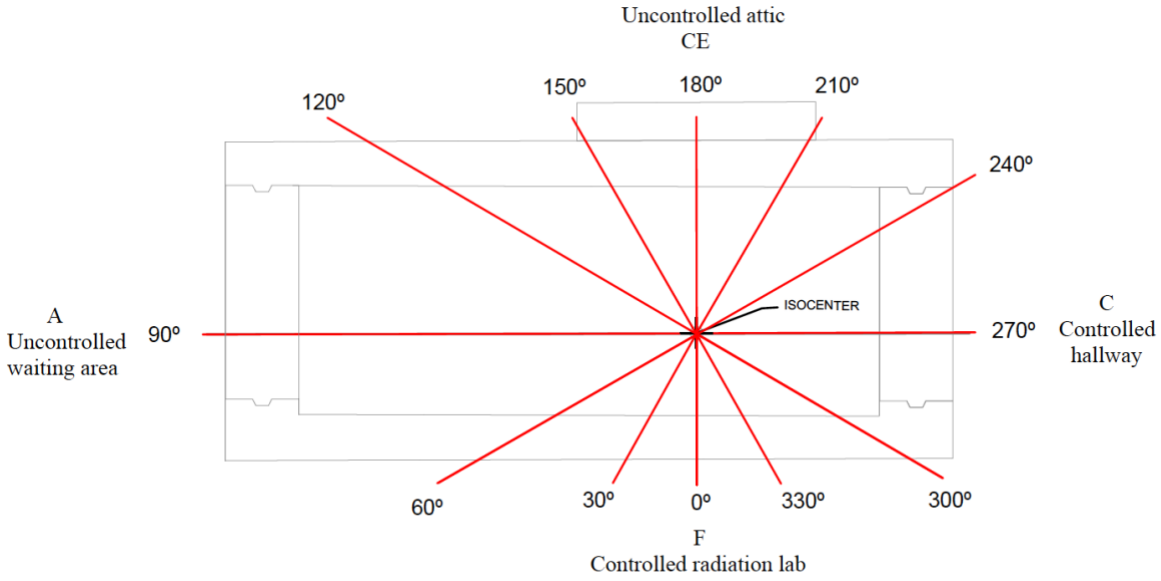

Figure 4.3. Front elevation view through isocenter of the sample vault layout. The red lines represent the center of the use factor angle intervals.

Compared to using the Report 151 IMRT use factor for the 45° interval centered at 180°, Table 4.5 shows that the VMAT use factor for this interval would save about 6 cm of concrete thickness across the width of the ceiling for an untapered barrier. The VMAT use factor is also better to use than an assumed uniform value for an untapered ceiling, although the savings in material is only 1 cm. Therefore, assuming uniformly distributed use factors for VMAT is adequate if designed an untapered ceiling. For a tapered ceiling design, Report 151 use factors yield an unsatisfactory barrier in all lateral segments of the ceiling. Report 151 underestimates the shielding requirements, resulting in an unsafe tapered barrier. By comparison, the assumption of uniformly use factors results in a tapered ceiling almost identical to the ceiling based on VMAT use factors.

Table 4.5. Comparison of barrier thicknesses in the ceiling (CE) when using 30º interval use factors for VMAT vs. uniformly distributed and 45º interval use factors from Report 151 vs uniformly distributed.

Barrier	VMAT		Uniform		Report 151	
	Use Factor	Thickness [cm]	Use Factor	Thickness [cm]	Use Factor	Thickness [cm]
CE-120º	0.083	62.1	0.083	62.1	0.040	56.8
CE-150º	0.082	118.8	0.083	119	0.040	109.9
CE-180º	0.077	139.3	0.083	140.4	0.23	155.0
CE-210º	0.081	118.6	0.083	118.9	0.058	114.4
CE-240º	0.080	64.5	0.083	64.8	0.058	62.2

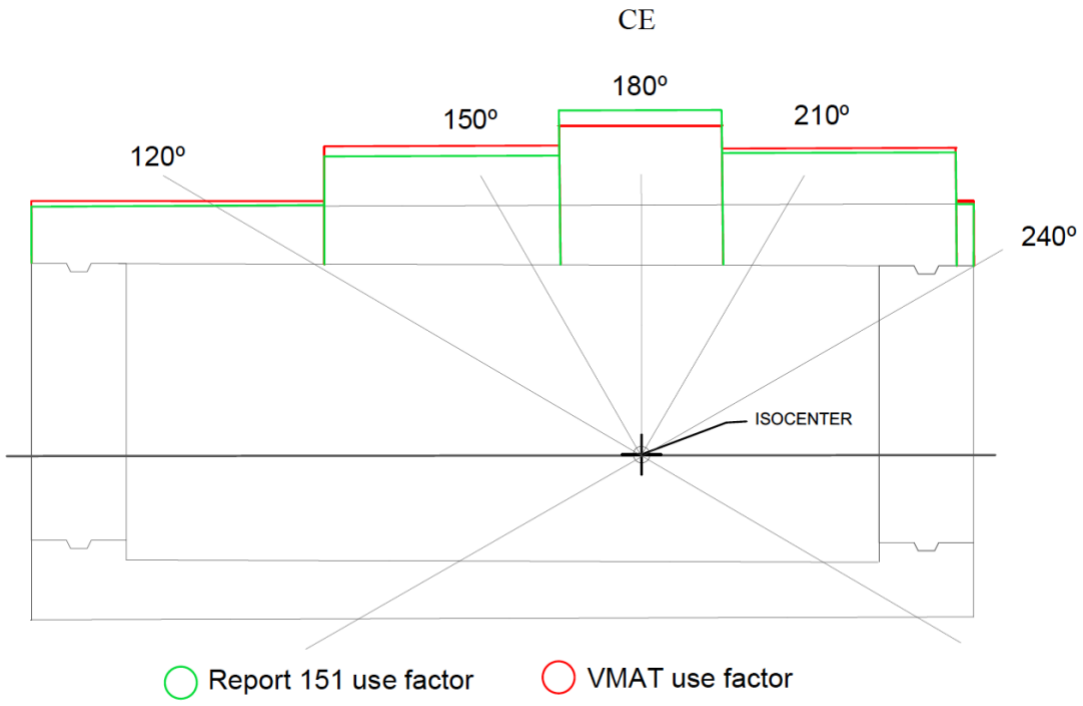

Figure 4.4. Front elevation floor plan showcasing the design of a tapered ceiling. Each slab represents the barrier thickness from the angle intervals in Table 4.5. The green lines represent the barrier design resulting from the assumption of Report 151 use factors, and the red lines represent the necessary thickness on the barriers to successfully shield for VMAT deliveries. NCRP successfully shields for the radiation incident at 180º (gantry pointing up) but yields an inadequate thickness for the rest of the slabs.

4.3. Other considerations for shielding design

4.3.1. Site specific use factors

The use factor analysis in Chapter 3 clearly indicated that the chest and lung treatment sites deviated the most from exhibiting a relatively uniform distribution of use factors. This section illustrates the potential negative impact of not using treatment site-specific use factors in the hypothetical situation of a vault that exclusively treats that site. Essentially, the question is whether barriers designed with the composite VMAT use factors will be sufficient if all the workload in the vault is delivered according to the chest site's distribution of use factors. Barrier thicknesses were calculated using 30º interval VMAT use factors derived solely from chest VMAT log files, and compared to the barrier thicknesses calculated from the composite VMAT use factors (Table 4.6). $H_{shielded}$ was calculated with the chest deliveries determining the $H_{unshielded}$ and the barrier's transmission factor determined from the VMAT barrier thickness.

Per the dose equivalent presented in Table 4.6, using the composite VMAT use factors (or similarly, assuming uniform distribution of use factors) to design a treatment vault that delivers only to the chest site would yield adequate barriers except for the floor. For this layout, the only instances where the floor was adequate were for the most oblique beams incident on that barrier. The floor region below isocenter would need additional concrete thickness to meet the design goal. While this specific situation of chest deliveries (not commonly done with VMAT) and floor (rarely a barrier with anything located below it) is rather contrived, it serves to illustrate that point that heavy utilization of a linac for a specific treatment site can impact shielding design, especially if the vault was designed for a more generalized case load. As Report 151 cautions, the qualified expert should consider the detailed situation and unique characteristics when designing vault shielding.

Table 4.6. Comparison of barrier thickness using VMAT and chest 30º interval use factors for all barriers, where $H_{shielded}$ represents the dose equivalent beyond the barrier when the chest workload is delivered through the composite-based barrier thickness.

Barrier	VMAT		Chest		P [μSv/week]	$H_{shielded}$ [μSv/week]
	Use Factor	Thickness [cm]	Use Factor	Thickness [cm]		
F-0º	0.096	162	0.123	166	100	127.44
F-30º	0.088	144	0.113	147	100	128.40
F-60º	0.082	82	0.086	83	100	20.91
A-90º	0.083	122	0.083	122	20	20.06
CE-120º	0.083	82	0.075	81	20	18.06
CE-150º	0.082	104	0.059	100	20	14.45
CE-180º	0.077	140	0.059	136	20	15.48
CE-210º	0.081	119	0.064	116	20	15.79
C-240º	0.080	75	0.067	74	20	16.77
C-270º	0.081	133	0.067	133	100	83.22
F-300º	0.080	65	0.082	65	100	101.88
F-330º	0.087	144	0.122	148	100	140.19

4.3.2. Secondary barriers, doors, and mazes

During the shielding design of a radiotherapy treatment vault, the qualified expert must design secondary barriers for leakage and patient scatter radiation, as well as consider door and maze design. The use factor distributions were the principle shielding parameter that was impacted by VMAT. Changes in workload affect all barriers, use factor is 1 by definition for secondary barriers, and the modulation factor for VMAT was found to be similar to that for IMRT; thus VMAT should not have a particular impact on secondary barriers.

With respect to door and maze design, Report 151 defines the dose equivalent at the maze entrance as a combined product of the secondary radiation due to primary radiation scattered from

the patient and walls, leakage radiation scattered from walls, and leakage radiation transmitted through the inner maze wall. As with secondary barriers, the amount of secondary radiation reaching the door is not impacted by VMAT use factors. In fact, door and maze design typically makes the assumption that gantry rotation is uniform (NCRP, 2005), so that the qualified expert can scale the contributions of the worst-case wall to account for other barriers' contributions. The relatively uniform distribution of VMAT use factors means that VMAT deliveries easily meet this assumption of uniform gantry rotation.

Chapter 5. Discussion and conclusion

5.1. Discussion

This work analyzed daily log files over a 4-month period for five Elekta linear accelerators at several facilities of the Mary Bird Perkins Cancer Center system. The analysis determined VMAT-specific shielding characteristics from mechanical state data recorded as the linacs delivered radiotherapy treatments. The log file data was characterized in terms of treatment-related metrics, such as parameters of the treatment arcs, prescribed dose, and treatment site. This data characterization can be used by qualified experts to assess the applicability of the results and recommendations of this work relative to their own facilities.

During the 4-month period, VMAT deliveries occurred on all five linacs. Several of the linacs had roughly equal amounts of VMAT vs. other types of deliveries, measured by machine MUs. Only one linac had VMAT treatments as the substantial majority of its deliveries. The weekly workloads derived from the log files for the linacs generally agreed with independent clinic records. With the expectation that four months of data for five linacs provided a representative snapshot of utilization, the supposition that a linac would be used exclusively for VMAT deliveries seems unlikely – certainly not for a small general-purpose facility with only one or two linacs. Conceivably at a large institution with many linacs, dedicating a linac to only VMAT treatments could be plausible.

The treatment site metric indicated that the sites treated most frequently with VMAT were pelvis, lung, and head & neck. While VMAT was utilized to some extent for all treatment sites, VMAT was the dominant choice of treatment method for each of these three sites. VMAT was used almost exclusively for treatment of the pelvis (median of 58 VMAT arcs out of 61 beams delivered, or 95%) and head and neck (median of 37 VMAT arcs out of 41 beams delivered, or

90%). This indicated that VMAT treatments on a particular linac could indeed be limited to one or a few sites; thus treatment-site specific VMAT utilization should be assessed by qualified experts for shielding design.

In prior literature, a VMAT modulation factor of 4.6 $\pm$1.6 was reported (Saleh et al., 2017). This modulation factor fell within the IQR of this study's data, which had a mean of 3.3 in this work. Report 151 noted that IMRT modulation factors typically fall in the range of 2-10 (NCRP, 2005). Modulation factor primarily impacts leakage barrier requirements, so VMAT is not expected to alter the design of secondary barriers in terms of leakage, compared to IMRT. Similarly, IMRT and VMAT deliver radiation to comparably-sized conformal treatment volumes, so the scattered radiation aspects will also be similar.

Composited over all accelerators and treatment sites, the use factors were computed for binning intervals of 90º, 45º, 30º, and 15º. The use factors were relatively uniformly distributed over the full circle of gantry motion, with deviations from uniform being the most noticeable at the smaller binning intervals and for the 0° (beam directed at floor) and 180° (beam directed at ceiling) gantry positions. Not surprisingly, the arc delivery style spread the radiation delivery relatively evenly. In the case of the beam directed at the ceiling, the discrepancy became more noticeable at smaller binning intervals due to the gantry never being truly at 180º to avoid mechanical collisions with the floor and treatment couch. Compared to Report 151, the VMAT use factors were smaller at 0º and 180º, but larger at 90º and 270º gantry positions. In retrospect this is not surprising: even though lateral beams may not be preferable due to longer pathlengths through normal tissue, they are used more frequently in VMAT to achieve conformality while minimizing dose to normal tissues (less dose, but delivered over a large volume with broad arcs). The sample calculations showed that using VMAT-specific use factors or even the simplified assumption of uniform gantry

rotation (a constant use factor at each interval) was consistently more likely to result in a safe barrier compared to the Report 151 use factors, especially for the 45° intervals. Qualified experts should not use the Report 151 use factors when designing shielding for VMAT vaults.

The use factors per treatment site were also relatively uniformly distributed, except for lung and chest sites. The observed asymmetries in distribution were likely due to the site's proximity to organs at risk in the thorax, especially contralateral lung. The sample calculations showed that for a vault dedicated to chest deliveries, areas in the floor could be inadequately shielded. Although the chest itself was not specifically interesting (the site was not prevalent for VMAT and the floor is rarely a concern due to vaults being routinely placed on the lowermost floor of a facility), this example emphasized that the characteristics of particular treatment sites may strongly impact the adequacy of a shielding design.

The sample calculations for vault shielding designs showed that the Report 151 use factors may underestimate barrier requirements for a vault used predominantly for VMAT. While the inclusion of substantial conservative margins on calculations should allow Report 151-based barriers to be adequately safe, further investigation would be needed to quantify the level of margin needed. Such designs would overshield the vault compared to the VMAT use factors or the assumption of uniform gantry rotation, potentially wasting money and material. The inadequacy of Report 151 use factors would be most likely to impact a tapered ceiling barrier design rather than walls or other barriers. Using the VMAT use factors or use factors derived from an assumption of uniform rotation should provide the best savings in materials while also ensuring a safe design.

5.1.1. Broader applicability of the current work

The independent analysis of the clinical records indicated good correspondence between the workload, use factor, and modulation factor results because a large pool of data was acquired.

Regardless, the extent of the generalization of the obtained data is still not understood and out of the scope of this project to characterize. This work included a detailed analysis of the weekly workload for the Mary Bird Perkins Cancer Center facilities, but this data was limited to a single manufacturer and two similar machine models. Regardless, substantial differences compared to other linac manufacturers and models, or to operations at other clinics, would seem unlikely; the spatial distribution of use factors and the modulation factors should be similar, as they are based on the same underlying physics, biology, and treatment goals. Regardless of the clinic, physician or dosimetrist, radiation transport and radiobiological effects dictate that treatment deliveries will be substantially similar across patients for each case type. The results presented here should be generally applicable across accelerator models and vendors; differences between facilities should be primarily due to differences in patient census, that is, the numbers of treatments to a particular tumor site or sites. Again, qualified experts must assess their particular circumstances to decide whether the results of this work should be used to represent their own clinical environment.

5.2. Conclusions

The use factors recommended in Report 151 are not guaranteed to provide safe barriers for linac vaults used heavily for VMAT, although sufficiently large conservative margins could potentially overcome the deficits. When designing the shielding for vaults that will be used predominately for VMAT, qualified experts should use VMAT-specific use factors. The VMAT-specific use factors reported in this work consistently led to primary barrier thicknesses that were at least as safe as those calculated from published Report 151 use factors. If VMAT-specific use factors are not available, the assumption of uniform gantry rotation (i.e., a constant use factor at each interval) is a reasonable alternative. Smaller (i.e., 30° or 45°) intervals for use factors result in thinner barriers than do larger (i.e., 90°) intervals, although smaller intervals would presumably

be more susceptible to variations in utilization or changes in VMAT delivery methods. Smaller intervals are attractive when designing a tapered ceiling barrier in a dedicated VMAT vault, and should result in a ceiling barrier that is safe while using less material; the 45° interval use factors from Report 151 should *not* be used to design a tapered ceiling barrier in a dedicated VMAT vault. Finally, if a vault will be used exclusively for VMAT, and especially for only one or a few treatment sites, the qualified expert should develop and use institution-specific treatment site-specific use factors or verify that composite VMAT use factors will be satisfactory.

The log file data for this work was accumulated over a four-month period for five linacs. This work has assumed this data to be representative of current practice. To ensure representative data, one should continue collecting log files for a long period, combining the additional data with the data reported here. For data that is representative of national practice, one should consider collecting data from multiple institutions. In addition, all linacs used in this work were Elekta Versa and Agility models. Again, to ensure representative data, VMAT-specific data should be collected for a wide range of vendors and models.

This work originally planned to make TLD measurements on barrier surfaces inside the linac vaults, to validate the workload and use factors derived from log files. TLD measurements could also be used to assess the magnitudes of secondary radiation at the barriers. Access restrictions due to the COVID pandemic, coupled to a failure of the TLD reader, prevented the incorporation of TLD measurements in this work. These validation measurements should be pursued in the future when opportunity permits.

Appendix A. Clinical metrics

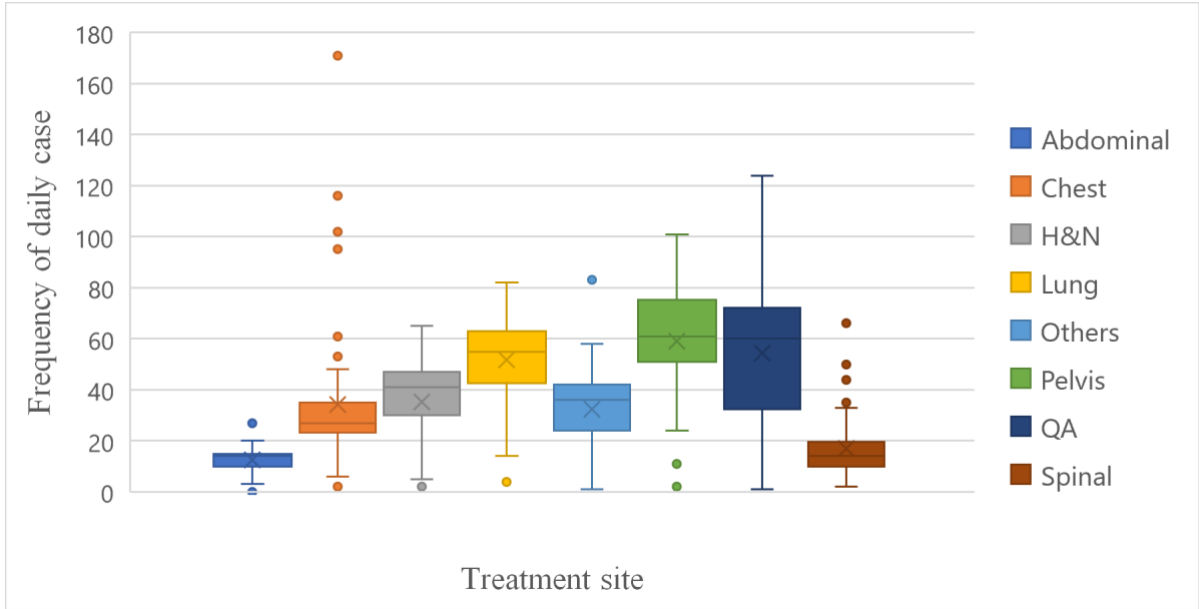

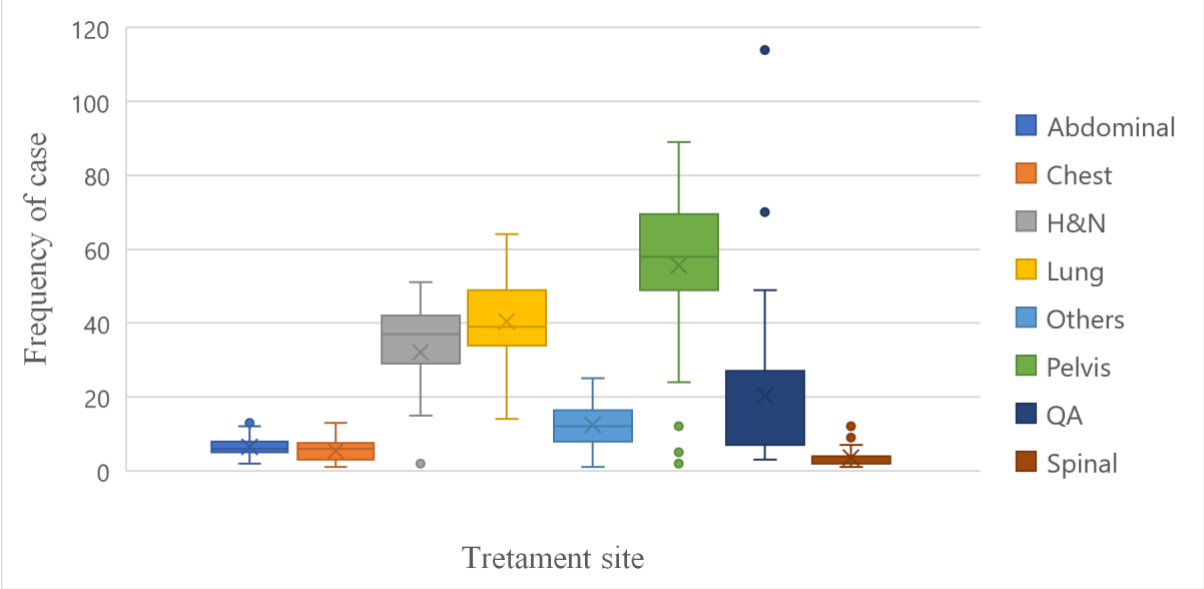

Figure A.1. Boxplot representation of the daily deliveries for (upper) all delivered beams and (lower) VMAT arcs only. The box sides represent interquartile range (IQR), this range contains 50% of the data points. The line within the IQR is the median, with the cross being the mean. The whiskers are the minimum and maximum values of the data range, and the outlying data points are the points greater or inferior to 1.5 times the IQR.

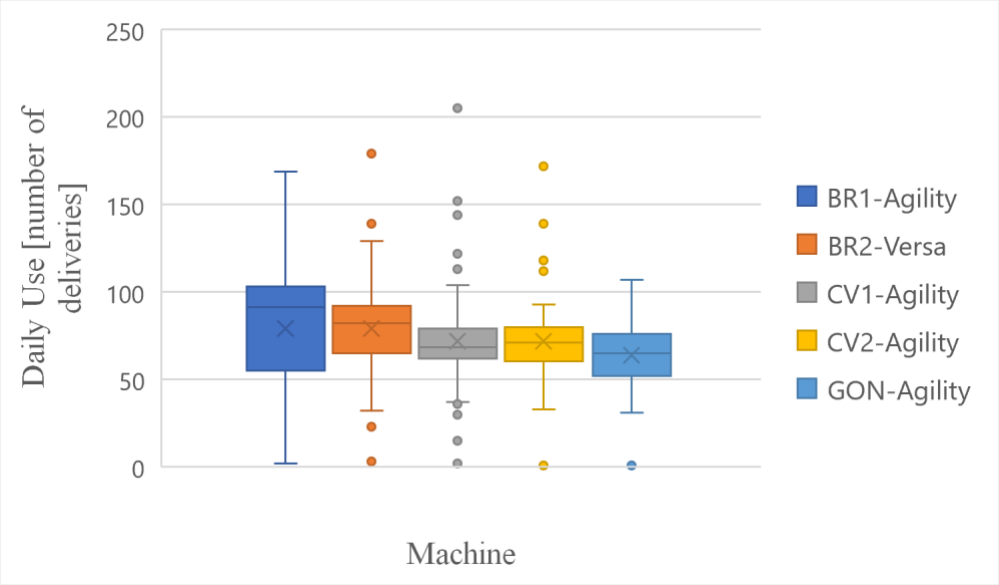

Figure A.2. Boxplot illustrating the frequency of machine usage for all delivery types, where the box sides represent interquartile range (IQR) which contains 50% of the data points. The line within the IQR is the median, with the cross marking the mean. The whiskers mark the minimum and maximum values of the data range, and the outlying data points are the points greater or inferior to 1.5 times the IQR.

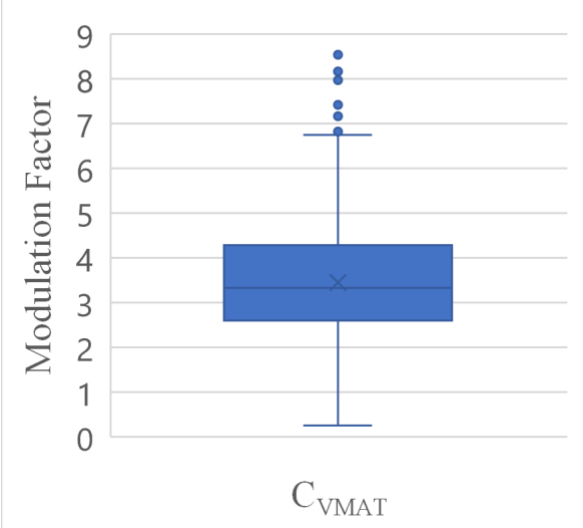

Figure A.3. Boxplot illustrating the VMAT modulation factor, where the box sides represent interquartile range (IQR) which contains 50% of the data points. The line within the IQR is the median, with the cross marking the mean. The whiskers mark the minimum and maximum values of the data range, and the outlying data points are the points greater or inferior to 1.5 times the IQR.

Appendix B. Use factors

Table B.1. Summary of VMAT use factors derived with intervals of 90°.

Bin	Frequency	Use Factor
0º	592958	0.271
90º	542831	0.248
180º	524399	0.240
270º	529026	0.242

Table B.2. Summary of the VMAT use factors derived with intervals of 45°.

Bin	Frequency	Use Factor
0º	310328	0.141
45º	279031	0.127
90º	272101	0.124
135º	272614	0.124
180º	257008	0.117
225º	264611	0.121
270º	265216	0.121
315º	273232	0.125

Table B.3. Summary of the VMAT use factors derived with intervals of 30°.

Bin	Frequency	Use Factor
0	210645	0.096
30	192467	0.088
60	179321	0.082
90	181765	0.083
120	181745	0.083
150	180013	0.082
180	168072	0.077
210	176314	0.081
240	175695	0.080
270	177502	0.081
300	175829	0.080
330	189846	0.087

Table B.4. Summary of the VMAT use factors derived with intervals of 15°.

Bin	Frequency	Use Factor
0	107157	0.049
15	101863	0.047
30	95806	0.044
45	93499	0.043
60	89012	0.041
75	89241	0.041
90	91028	0.042
105	91056	0.042
120	91414	0.042
135	88771	0.041
150	91768	0.042
165	91651	0.042
180	73868	0.034
195	91088	0.042
210	88059	0.041
225	88620	0.041
240	87386	0.040
255	88135	0.040
270	89201	0.041
285	87287	0.040
300	87918	0.040
315	89420	0.041
330	95253	0.044
345	100713	0.046

Table B.5. Angular mean, median and IQR of the data distribution for 90º angle intervals. The data is shown as a boxplot in Figure B.1.

Bin	Mean	Median	IQR
0º	0.3	0.3	[338.7, 21.8]
90º	90.1	90.3	[67.6,112.7]
180º	179.8	176.1	[135.1, 202.7]
270º	270.1	270.0	[247.6, 292.6]

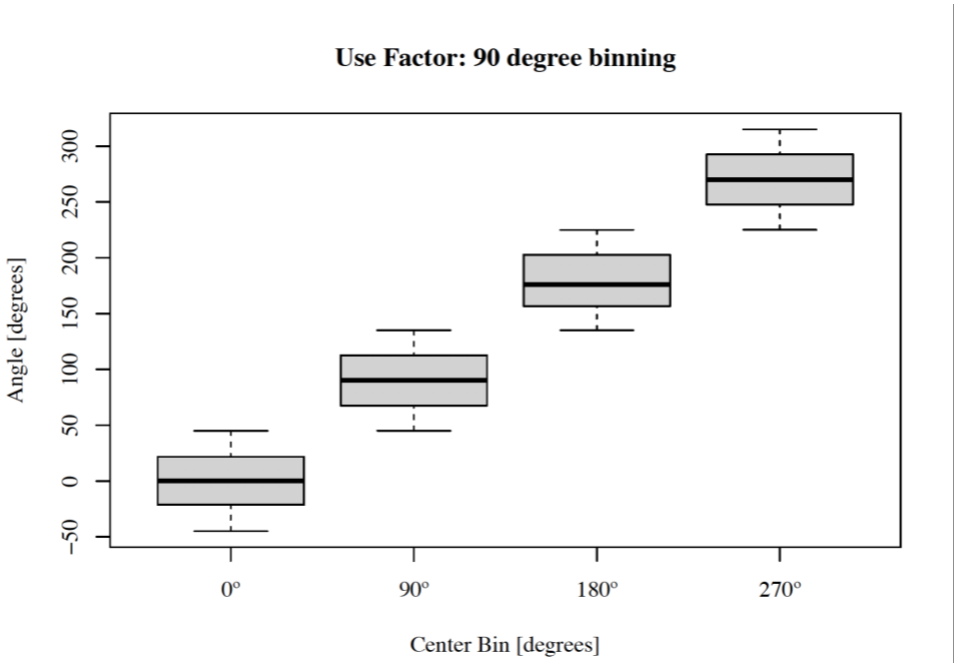

Figure B.1. Boxplot illustrating the angle bin data at 90º angular intervals, where the box sides represent interquartile range (IQR) which contains 50% of the data points. The line within the IQR is the median, with the cross marking the mean. The whiskers mark the minimum and maximum values of the data range.

Table B.6. Angular mean, median and IQR of the data distribution for 45º angle interval. The data is shown as a boxplot in Figure B.2.

Bin	Mean	Median	IQR
0º	0.08	0.1	[349.2, 10.9]
45º	44.6	44.5	[33.3, 55.8]
90º	90.2	90.2	[79.0, 101.4]
135º	135.0	135.0	[123.7, 146.4]
180º	180.0	180.6	[168.3, 191.9]
225º	225.0	225.0	[213.8, 236.2]
270º	270.0	269.9	[258.8, 281.2]
315º	315.5	315.7	[304.2, 326.8]

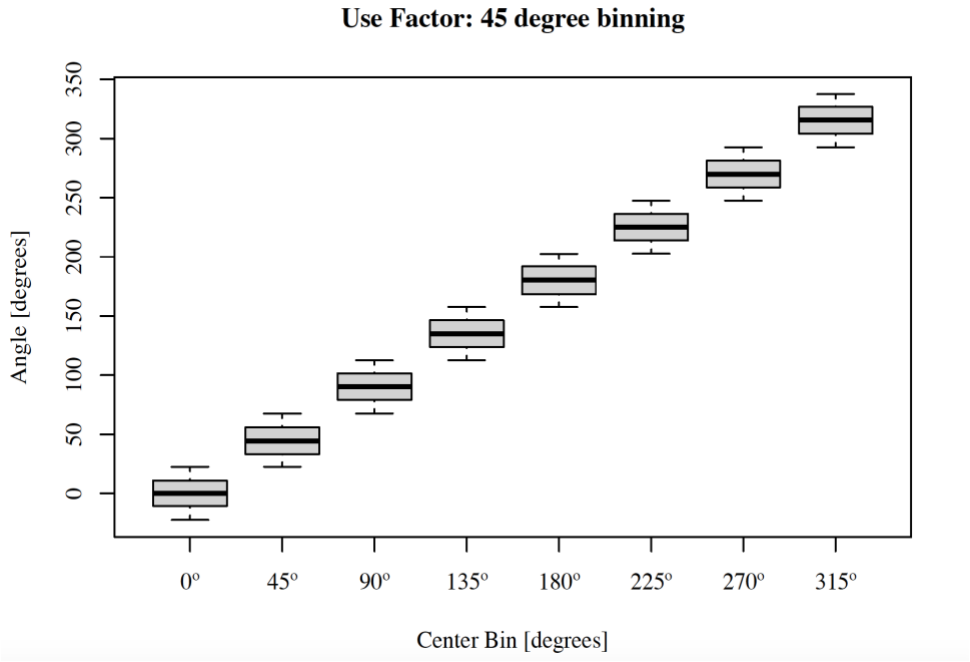

Figure B.2. Boxplot illustrating the angle bin data at 45º angular intervals, where the box sides represent interquartile range (IQR) which contains 50% of the data points. The line within the IQR is the median, with the cross marking the mean. The whiskers mark the minimum and maximum values of the data range.

Table B.7. Angular mean, median and IQR of the data distribution in 30º angle intervals. The data is shown as a boxplot in Figure B.3.

Bin	Mean	Median	IQR
0º	0.12	0.1	[352.8, 7.5]
30º	29.8	29.7	[22.4, 37.4]
60º	59.9	59.8	[52.3, 67.4]
90º	90.1	90.1	[82.6, 97.6]
120º	120.0	120.0	[112.5, 127.4]
150º	157.4	150.1	[142.7, 157.4]
180º	180.0	180.4	[171.8, 188.3]
210º	210.0	210.1	[202.5, 217.5]
240º	240.0	240.0	[232.5, 247.5]
270º	270.0	269.9	[262.6, 277.5]
300º	300.1	300.2	[292.6, 307.7]
330º	330.3	330.3	[322.9, 337.8]

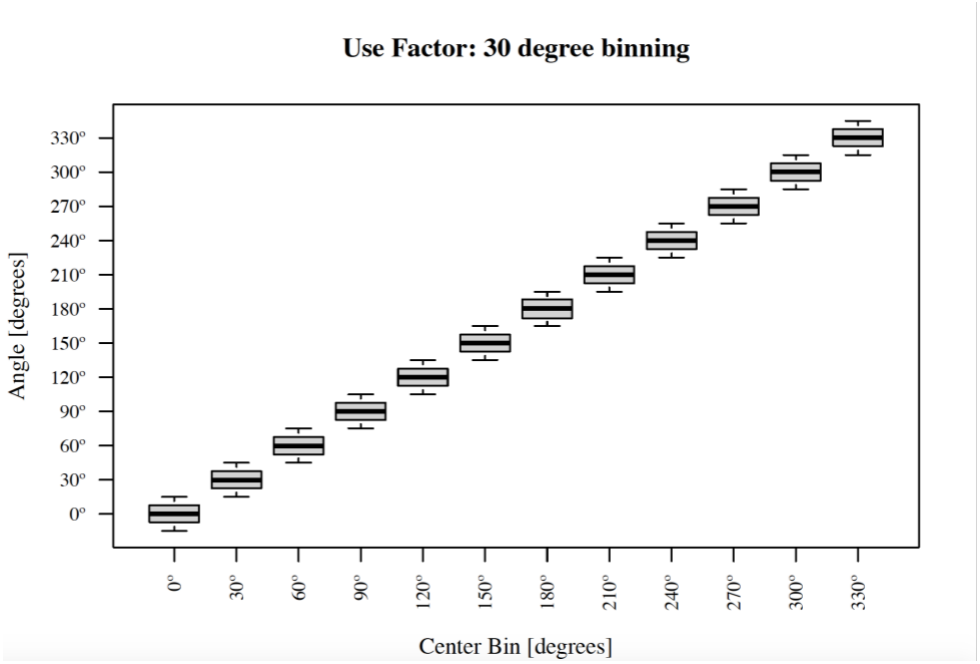

Figure B.3. Boxplot illustrating the angle bin data at 30º angular intervals, where the box sides represent interquartile range (IQR) which contains 50% of the data points. The line within the IQR is the median, with the cross marking the mean. The whiskers mark the minimum and maximum values of the data range.

Table B.8. Angular mean, median and IQR of the data distribution in 30º angle intervals. The data is shown as a boxplot in Figure B.4.

Bin	Mean	Median	IQR
0º	0.05	0.1	[356.3, 3.8]
15º	15.0	14.8	[11.2, 18.6]
30º	29.9	29.8	[26.2, 33.6]
45º	45.0	45.0	[41.3, 48.7]
60º	60.0	60.0	[56.2, 63.8]
75º	75.1	75.2	[71.4, 78.8]
90º	90.1	90.1	[86.4, 93.8]
105º	105.0	105.0	[101.3, 108.9]
120º	120.1	120.0	[116.2, 123.8]
135º	135.0	135.1	[131.3, 138.7]
150º	150.0	150.0	[146.3, 153.7]
165º	165.2	165.3	[161.5, 169.1]
180º	180.0	180.7	[174.8, 185.2]
195º	194.9	194.8	[191.1, 198.6]
210º	210.1	210.1	[206.3, 213.8]
225º	225.0	225.1	[221.3, 228.8]
240º	240.0	240.1	[236.3, 243.8]
255º	255.1	255.1	[251.4, 258.8]
270º	270.0	270.0	[266.3, 273.7]
285º	285.0	285.0	[281.4, 288.8]
300º	300.1	300.1	[296.3, 303.8]
315º	315.1	315.1	[311.4, 318.8]
330º	330.1	330.1	[326.3, 333.8]
345º	345.0	345.0	[342.2, 348.9]

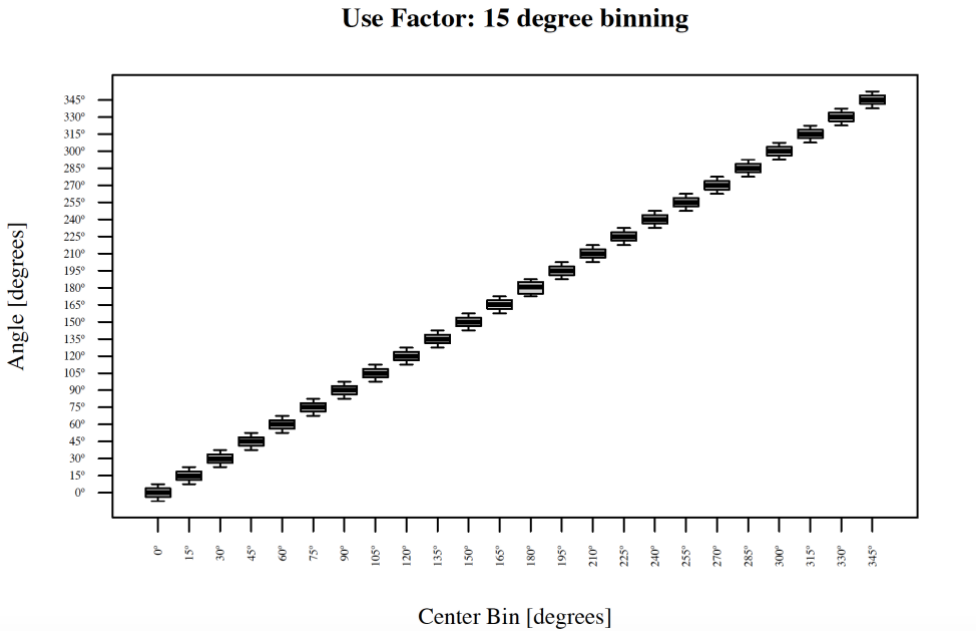

Figure B.4. Boxplot illustrating the angle bin data at 15º angular intervals, where the box sides represent interquartile range (IQR) which contains 50% of the data points. The line within the IQR is the median, with the cross marking the mean. The whiskers mark the minimum and maximum values of the data range.

Table B.9. Summary of the abdomen VMAT use factors for angle intervals of 90º, 45º, 30º, 15º.

90º angle interval		45º angle interval		30º angle interval		15º angle interval	
0º	0.265	0º	0.134	0º	0.090	0º	0.044
90º	0.260	45º	0.129	30º	0.087	15º	0.045
180º	0.242	90º	0.132	60º	0.085	30º	0.044
270º	0.232	135º	0.130	90º	0.089	45º	0.043
		180º	0.120	120º	0.086	60º	0.043
		225º	0.116	150º	0.087	75º	0.043
		270º	0.116	180º	0.078	90º	0.044
		315º	0.124	210º	0.077	105º	0.044
				240º	0.077	120º	0.043
				270º	0.078	135º	0.044
				300º	0.077	150º	0.042
				330º	0.088	165º	0.044
						180º	0.037
						195º	0.039
						210º	0.039
						225º	0.039
						240º	0.039
						255º	0.039
						270º	0.038
						285º	0.039
						300º	0.038
						315º	0.044
						330º	0.042
						345º	0.045

Table B.10. Summary of the chest VMAT use factors for angle intervals of 90º, 45º, 30º, 15º.

90º angle interval		**45º angle interval**		**30º angle interval**		**15º angle interval**	
0º	0.357	0º	0.183	0º	0.123	0º	0.064
90º	0.244	45º	0.150	30º	0.113	15º	0.060
180º	0.182	90º	0.126	60º	0.086	30º	0.058
270º	0.217	135º	0.097	90º	0.083	45º	0.049
		180º	0.090	120º	0.075	60º	0.043
		225º	0.098	150º	0.059	75º	0.040
		270º	0.104	180º	0.059	90º	0.040
		315º	0.154	210º	0.064	105º	0.046
				240º	0.067	120º	0.036
				270º	0.067	135º	0.031
				300º	0.082	150º	0.030
				330º	0.122	165º	0.031
						180º	0.026
						195º	0.032
						210º	0.032
						225º	0.033
						240º	0.033
						255º	0.035
						270º	0.033
						285º	0.035
						300º	0.041
						315º	0.044
						330º	0.069
						345º	0.059

Table B.11. Summary of the head & neck VMAT use factors for angle intervals of 90º, 45º, 30º, 15º.

90º angle interval		**45º angle interval**		**30º angle interval**		**15º angle interval**	
0º	0.276	0º	0.145	0º	0.100	0º	0.052
90º	0.226	45º	0.122	30º	0.087	15º	0.047
180º	0.248	90º	0.110	60º	0.076	30º	0.044
270º	0.250	135º	0.118	90º	0.073	45º	0.041
		180º	0.121	120º	0.077	60º	0.038
		225º	0.130	150º	0.080	75º	0.037
		270º	0.123	180º	0.079	90º	0.036
		315º	0.129	210º	0.089	105º	0.037
				240º	0.084	120º	0.038
				270º	0.082	135º	0.039
				300º	0.084	150º	0.041
				330º	0.089	165º	0.041
						180º	0.033
						195º	0.047
						210º	0.044
						225º	0.044
						240º	0.042
						255º	0.041
						270º	0.041
						285º	0.041
						300º	0.042
						315º	0.043
						330º	0.044
						345º	0.047

Table B.12. Summary of the lung VMAT use factors for angle intervals of 90º, 45º, 30º, 15º.

90º angle interval		45º angle interval		30º angle interval		15º angle interval	
0º	0.290	0º	0.160	0º	0.110	0º	0.055
90º	0.284	45º	0.143	30º	0.096	15º	0.052
180º	0.238	90º	0.138	60º	0.095	30º	0.047
270º	0.188	135º	0.148	90º	0.092	45º	0.049
		180º	0.117	120º	0.097	60º	0.047
		225º	0.095	150º	0.098	75º	0.046
		270º	0.092	180º	0.077	90º	0.046
		315º	0.108	210º	0.063	105º	0.046
				240º	0.062	120º	0.050
				270º	0.062	135º	0.047
				300º	0.064	150º	0.051
				330º	0.084	165º	0.050
						180º	0.033
						195º	0.034
						210º	0.031
						225º	0.032
						240º	0.031
						255º	0.030
						270º	0.031
						285º	0.031
						300º	0.033
						315º	0.032
						330º	0.043
						345º	0.052

Table B.13. Summary of the others VMAT use factors for angle intervals of 90º, 45º, 30º, 15º.

90º angle interval		**45º angle interval**		**30º angle interval**		**15º angle interval**	
0º	0.280	0º	0.143	0º	0.095	0º	0.049
90º	0.228	45º	0.126	30º	0.094	15º	0.048
180º	0.229	90º	0.116	60º	0.074	30º	0.049
270º	0.264	135º	0.111	90º	0.079	45º	0.041
		180º	0.112	120º	0.075	60º	0.037
		225º	0.128	150º	0.072	75º	0.038
		270º	0.137	180º	0.074	90º	0.040
		315º	0.128	210º	0.084	105º	0.038
				240º	0.088	120º	0.038
				270º	0.093	135º	0.036
				300º	0.083	150º	0.036
				330º	0.090	165º	0.035
						180º	0.033
						195º	0.044
						210º	0.042
						225º	0.042
						240º	0.043
						255º	0.047
						270º	0.046
						285º	0.044
						300º	0.041
						315º	0.042
						330º	0.045
						345º	0.046

Table B.14. Summary of the pelvis VMAT use factors for angle intervals of 90º, 45º, 30º, 15º.

90º angle interval		**45º angle interval**		**30º angle interval**		**15º angle interval**	
0º	0.251	0º	0.128	0º	0.087	0º	0.049
90º	0.254	45º	0.123	30º	0.082	15º	0.044
180º	0.239	90º	0.130	60º	0.082	30º	0.043
270º	0.256	135º	0.124	90º	0.088	45º	0.040
		180º	0.117	120º	0.084	60º	0.041
		225º	0.125	150º	0.081	75º	0.041
		270º	0.130	180º	0.076	90º	0.042
		315º	0.125	210º	0.082	105º	0.044
				240º	0.085	120º	0.043
				270º	0.088	135º	0.042
				300º	0.084	150º	0.040
				330º	0.083	165º	0.041
						180º	0.041
						195º	0.035
						210º	0.041
						225º	0.041
						240º	0.041
						255º	0.042
						270º	0.043
						285º	0.044
						300º	0.042
						315º	0.042
						330º	0.042
						345º	0.041

Table B.15. Summary of the QA VMAT use factors for angle intervals of 90º, 45º, 30º, 15.

90º angle interval		**45º angle interval**		**30º angle interval**		**15º angle interval**	
0º	0.260	0º	0.135	0º	0.091	0º	0.046
90º	0.245	45º	0.124	30º	0.083	15º	0.045
180º	0.242	90º	0.122	60º	0.083	30º	0.041
270º	0.253	135º	0.122	90º	0.082	45º	0.041
		180º	0.114	120º	0.080	60º	0.041
		225º	0.129	150º	0.083	75º	0.040
		270º	0.123	180º	0.072	90º	0.042
		315º	0.130	210º	0.087	105º	0.041
				240º	0.083	120º	0.040
				270º	0.084	135º	0.040
				300º	0.086	150º	0.042
				330º	0.086	165º	0.040
						180º	0.030
						195º	0.045
						210º	0.044
						225º	0.043
						240º	0.042
						255º	0.040
						270º	0.041
						285º	0.043
						300º	0.044
						315º	0.044
						330º	0.042
						345º	0.044

Table B.16. Summary of the spine VMAT use factors for angle intervals of 90º, 45º, 30º, 15º.

90º angle interval		**45º angle interval**		**30º angle interval**		**15º angle interval**	
0º	0.255	0º	0.131	0º	0.090	0º	0.048
90º	0.266	45º	0.134	30º	0.092	15º	0.048
180º	0.247	90º	0.143	60º	0.087	30º	0.046
270º	0.231	135º	0.126	90º	0.097	45º	0.043
		180º	0.120	120º	0.082	60º	0.043
		225º	0.111	150º	0.087	75º	0.045
		270º	0.120	180º	0.085	90º	0.050
		315º	0.115	210º	0.076	105º	0.046
				240º	0.074	120º	0.041
				270º	0.081	135º	0.039
				300º	0.076	150º	0.044
				330º	0.074	165º	0.048
						180º	0.038
						195º	0.040
						210º	0.037
						225º	0.038
						240º	0.036
						255º	0.041
						270º	0.040
						285º	0.039
						300º	0.039
						315º	0.036
						330º	0.037
						345º	0.037

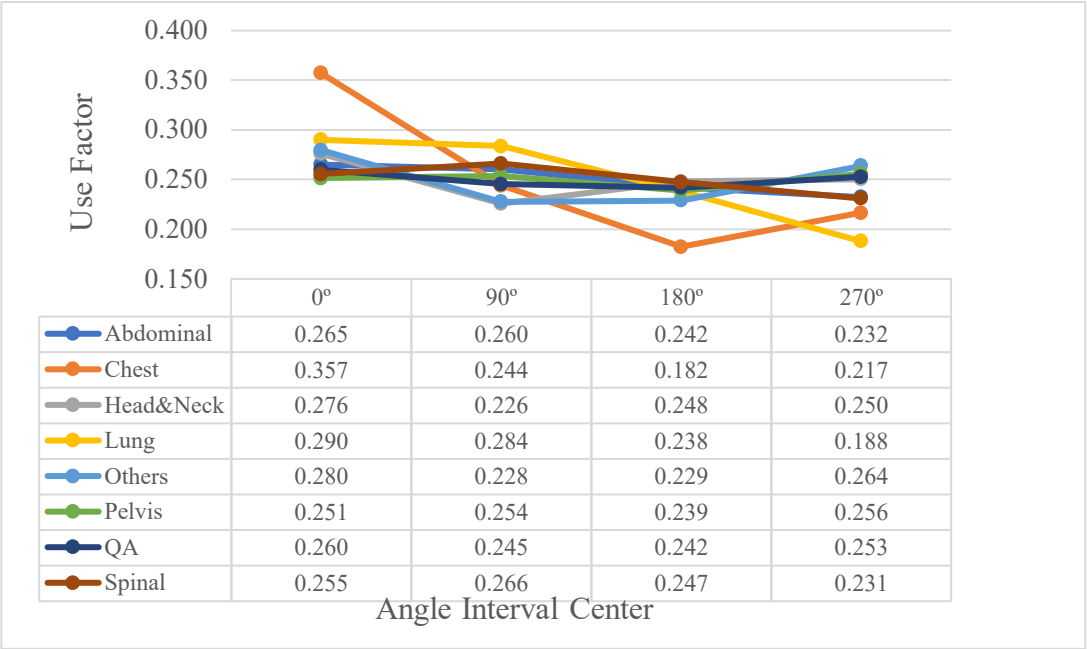

	0º	90º	180º	270º
Abdominal	0.265	0.260	0.242	0.232
Chest	0.357	0.244	0.182	0.217
Head&Neck	0.276	0.226	0.248	0.250
Lung	0.290	0.284	0.238	0.188
Others	0.280	0.228	0.229	0.264
Pelvis	0.251	0.254	0.239	0.256
QA	0.260	0.245	0.242	0.253
Spinal	0.255	0.266	0.247	0.231

Figure B.5. VMAT use factors at 90º intervals for each treatment site. This is the same data as shown in the radar plots of Figure 3.6, but shown as overlays for easier comparison.

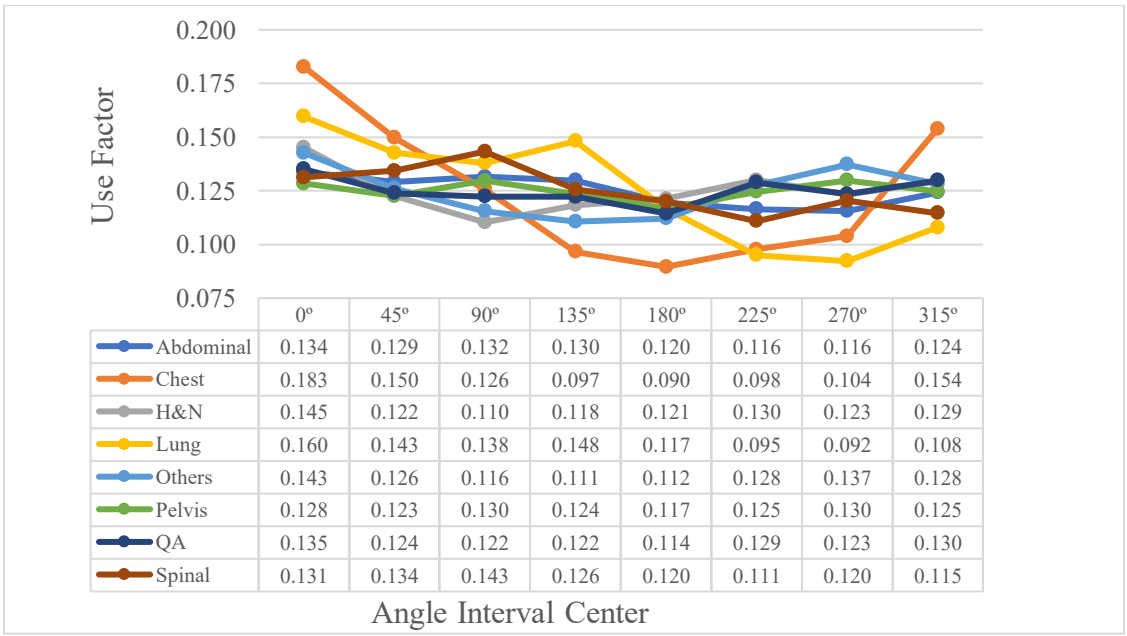

	0º	45º	90º	135º	180º	225º	270º	315º
Abdominal	0.134	0.129	0.132	0.130	0.120	0.116	0.116	0.124
Chest	0.183	0.150	0.126	0.097	0.090	0.098	0.104	0.154
H&N	0.145	0.122	0.110	0.118	0.121	0.130	0.123	0.129
Lung	0.160	0.143	0.138	0.148	0.117	0.095	0.092	0.108
Others	0.143	0.126	0.116	0.111	0.112	0.128	0.137	0.128
Pelvis	0.128	0.123	0.130	0.124	0.117	0.125	0.130	0.125
QA	0.135	0.124	0.122	0.122	0.114	0.129	0.123	0.130
Spinal	0.131	0.134	0.143	0.126	0.120	0.111	0.120	0.115

Figure B.6. VMAT use factors at 45º intervals for each treatment site. This is the same data as shown in the radar plots of Figure 3.6, but shown as overlays for easier comparison.

References

Benedict, S. H., Yenice, K. M., Followill, D., Galvin, J. M., Hinson, W., Kavanagh, B., … Yin, F. F. (2010). Stereotactic body radiation therapy: The report of AAPM Task Group 101. *Medical Physics*, *37*(8), 4078–4101. https://doi.org/10.1118/1.3438081

Grossman, L. I. (1982). A brief history of endodontics. *Journal of Endodontics*, *8*, S36–S40. https://doi.org/https://doi.org/10.1016/S0099-2399(82)80304-X

Inkret, W. C., Meinhold, C. B., & Taschner, J. C. (1995). Protection Standards. *Los Alamos Science*, *23*, 116–123. Retrieved from https://fas.org/sgp/othergov/doe/lanl/00326631.pdf

Kermani, P., Leclerc, G., Martel, R., & Fareh, J. (2001). Room shielding for intensity-modulated radiation therapy treatment facilities. *International Journal of Radiation Oncology Biology Physics*, *50*(1), 239–246. https://doi.org/10.1016/S0360-3016(01)01463-8

Khan, F. M. (2014). *The Physics of Radiation Therapy* (5th ed.). Philadelphia: Lippincott Williams & Wilkins.

Massart, D. L., Smeyers-Verbeke, J., Capron, X., & Schlesier, K. (2005). Visual presentation of data by means of box plots. *LC-GC Europe*, *18*(4), 215–218.

McDermott, P. N. (2007). Radiation shielding for gamma stereotactic radiosurgery units. *Journal of Applied Clinical Medical Physics*, *8*(3), 147–157. https://doi.org/10.1120/jacmp.v8i3.2355

Mechalakos, J. G., Germain, J. St., & Burman, C. M. (2004). Results of a one year survey of output for linear accelerators using IMRT and non-IMRT techniques. *Journal of Applied Clinical Medical Physics*, *5*(1), 64–72. https://doi.org/10.1120/jacmp.v5i1.1960

National Council on Radiation Protection and Measurements. (1976). *Structural shielding design and evaluation for medical use of X-rays and gamma rays of energies up to 10 MeV : recommendations of the National Council on Radiation Protection and Measurements.*

National Council on Radiation Protection and Measurements DC (USA), W. (1977). *Radiation protection design guidelines for 0.1 to 100 MeV particle accelerator facilities*. United States. Retrieved from http://inis.iaea.org/search/search.aspx?orig_q=RN:09379508

NCRP. (1986). *Neutron Contamination from Medical Electron Accelerators (NCRP Report No. 79)*. *NCRP Report* (Vol. 13). https://doi.org/10.1118/1.595800

NCRP. (1989). Medical X-ray, electron beam and gamma-ray protection for energies up to 50 MeV. (Equipment design, performance and use). *NCRP Report*, (102), 1–117.

NCRP. (1993). *National Council on Radiation Protection and Measurements. Limitation of Exposure to Ionizing Radiation, NCRP Report No. 116*. *National Council on Radiation Protection and Measurements* (Vol. 35). Bethesda, Maryland. https://doi.org/10.1177/028418519403500628

NCRP. (2005). *Structural Shielding Design and Evaluation for Megavoltage X- and Gamma-Ray Radiotherapy Facilities, NCRP Report No. 151*. *Health Physics* (Vol. 91). https://doi.org/10.1097/01.hp.0000205229.89321.ce

NCRP. (2019). *NCRP Annual Report. 2020 Year in Review*. *Annual Report* (Vol. 54). https://doi.org/10.1016/j.jcjo.2019.06.003

Otto, K. (2008). Volumetric modulated arc therapy: IMRT in a single gantry arc. *Medical Physics*, *35*(1), 310–317. https://doi.org/10.1118/1.2818738

Reis, J. P., Alves, V. G., & Fairbanks, L. R. (2019). Total Workload for Radioactive Facilities with Volumetric Modulated Arc Treatment. *Brazilian Journal of Radiation Sciences*, *7*(3). https://doi.org/10.15392/bjrs.v7i3.928

Robinson, D., Scrimger, J. W., Field, G. C., & Fallone, B. G. (2000). Shielding considerations for tomotherapy. *Medical Physics*, *27*(10), 2380–2384. https://doi.org/10.1118/1.1308281

Rodgers, J. E. (2005). CyberKnife Treatment Room Design and Radiation Protection. *Robotic Radiosurgery - Volume 1*, 41. Retrieved from www.cksociety.org

Saleh, Z. H., Jeong, J., Quinn, B., Mechalakos, J., St. Germain, J., & Dauer, L. T. (2017). Results of a 10-year survey of workload for 10 treatment vaults at a high-throughput comprehensive cancer center. *Journal of Applied Clinical Medical Physics*, *18*(3), 207–214. https://doi.org/10.1002/acm2.12076

Subpart D—Radiation Dose Limits For Individual Members Of The Public. (n.d.). Retrieved June 1, 2021, from https://www.nrc.gov/reading-rm/doc-collections/cfr/part020/part020-1301.html

Teoh, M., Clark, C. H., Wood, K., Whitaker, S., & Nisbet, A. (2011). Volumetric modulated arc therapy: A review of current literature and clinical use in practice. *British Journal of Radiology*, *84*(1007), 967–996. https://doi.org/10.1259/bjr/22373346

Yu, C. X. (1995). Intensity-modulated arc therapy with dynamic multileaf collimation: an alternative to tomotherapy. *Physics in Medicine and Biology*, *40*(9), 1435–1449. https://doi.org/10.1088/0031-9155/40/9/004

Yu, C. X., & Tang, G. (2011, March 7). Intensity-modulated arc therapy: Principles, technologies and clinical implementation. *Physics in Medicine and Biology*. Phys Med Biol. https://doi.org/10.1088/0031-9155/56/5/R01

Vita

Ana Dieguez was born in Guatemala City, Guatemala in 1995. Ana lived in Guatemala City and attended high school in Colegio Monte Maria, graduating in 2012. In 2013, she enrolled in Universidad del Valle de Guatemala to pursue a career in physics, graduating with a undergraduate thesis titled “The design of a radiotelescope”. After graduating from Universidad del Valle, she enrolled in LSU’s Medical Physics Master of Science program. Following her graduation, she will begin a medical physics residency in Oregon Health and Science University.